AD-771 135

INTENSITY INTERFEROMETRY IN THE SPATIAL DOMAIN

Paul H. Deitz

Ballistic Research Laboratories
Aberdeen Proving Ground, Maryland

November 1973

ACCESSION for

NTIS   White Section   ☑
DDC   Buff Section   ☐
UNANNOUNCED   ☐
JUSTIFICATION

BY
DISTRIBUTION/AVAILABILITY CODES
Dist.   AVAIL. and/or SPECIAL

A

DOCUMENT CONTROL DATA - R & D

(Security classification of title, body of abstract and indexing annotation must be entered when the overall report is classified)

1 ORIGINATING ACTIVITY (Corporate author)	2a. REPORT SECURIT CLASSIFICATION
US Army Ballistic Research Laboratories Aberdeen Proving Ground, Maryland 21005	UNCLASSIFIED
	2b. GROUP

3 REPORT TITLE

INTENSITY INTERFEROMETRY IN THE SPATIAL DOMAIN

4 DESCRIPTIVE NOTES (Type of report and inclusive dates)

5 AUTHOR(S) (First name, middle initial, last name)

Paul H. Deitz

6 REPORT DATE	7a. TOTAL NO. OF PAGES	7b. NO. OF REFS
November 1973	73	29
8a. CONTRACT OR GRANT NO.	9a. ORIGINATOR'S REPORT NUMBER(S)	
b. PROJECT NO. RDT&E 1M562603A286	BRL Report No. 1687	
c.	9b. OTHER REPORT NO(S) (Any other numbers that may be assigned this report)	
d.		

10 DISTRIBUTION STATEMENT

Approved for public release; distribution unlimited.

11. SUPPLEMENTARY NOTES	12. SPONSORING MILITARY ACTIVITY
	US Army Materiel Command 5001 Eisenhower Avenue Alexandria, Virginia 22304

13 ABSTRACT

A modification of the Hanbury Brown-Twiss experiment is described whereby intensity correlation is performed using coherent light and the statistical averages are taken in the space domain. This result is used to reconstruct the irradiance distribution of a spatially rough source. The far-field intensity distribution is recorded spatially for one time-resolution unit of the detector. The resulting spatial signal is autocorrelated and related to the intensity distribution over the source. Thus, without averaging in the time domain, a spatial Fourier transform relation is derived between the far-field intensity correlation and the source irradiance, similar to the results of Hanbury Brown and Twiss.

A major limitation of intensity interferometry in both the space and time domains has been that only sources of even symmetry could be uniquely inferred from far-field intensity correlations, since only the modulus was derived. However, this restriction can be removed by processing, in addition, the field in a simple way before detection to form a new symmetrized function. Using the modulus of the total transform together with the real part of the transform, one can infer the phase to within a sign. Thus a pair of images is derived, one erect, the other inverted.

Finally, experimental evidence is offered to support the spatial transform relations predicted here.

DD FORM 1473 REPLACES DD FORM 1473, 1 JAN 64, WHICH IS OBSOLETE FOR ARMY USE.

14 KEY WORDS	LINK A		LINK B		LINK C	
	ROLE	WT	ROLE	WT	ROLE	WT
Coherence						
Interferometry						
Atmospheric Optics						
Scintillation						

BALLISTIC RESEARCH LABORATORIES

REPORT NO. 1687

NOVEMBER 1973

INTENSITY INTERFEROMETRY IN THE SPATIAL DOMAIN

Paul H. Deitz

Concepts Analysis Laboratory

The research reported here was conducted in
partial fulfillment of the requirements for
the degree of Doctor of Philosophy in the field
of Electrical Engineering, University of
Washington, December 1973.

ABERDEEN PROVING GROUND, MARYLAND

l

B A L L I S T I C   R E S E A R C H   L A B O R A T O R I E S

REPORT NO. 1687

PHDeitz/smj
Aberdeen Proving Ground, MD
November 1973

INTENSITY INTERFEROMETRY IN THE SPATIAL DOMAIN

ABSTRACT

Intensity interferometry, as developed by Hanbury Brown and Twiss
for stellar observation, has shown relative insensitivity to atmospheric
scintillation. However, with classical sources, the limitations placed
on this technique by quantum noise and detector efficiency are severe.
This situation is vastly improved when laser illumination is employed.
A modification of the Hanbury Brown - Twiss experiment is described whereby
intensity correlation is performed using coherent light and the statis-
tical averages are taken in the space domain. Generalizing a form of
the mutual coherence function, the far-zone behavior of the mutual inten-
sity function for an intermediate time average is derived. This result
is used to reconstruct the irradiance distribution of a spatially rough
source. The far-field intensity distribution is recorded spatially for
one time-resolution unit of the detector. The resulting spatial signal
is autocorrelated and related to the intensity distribution over the
source. Thus, without averaging in the time domain, a spatial Fourier-
transform relation is derived between the far-field intensity correlation
and the source irradiance, similar to the results of Hanbury Brown and
Twiss.

A major limitation of intensity interferometry in both the space
and time domains has been that only sources of even symmetry could be
uniquely inferred from far-field intensity correlations, since only the
modulus was derived. However, this restriction can be removed by pro-
cessing, in addition, the field in a simple way before detection to form
a new symmetrized function. This intensity record corresponds to the
radiation pattern derived from the pure even part of the intensity pro-
file. The record is autocorrelated, as before, yielding a spatial power
spectrum. But by the central-ordinate and hermitian properties of the
spatial Fourier transform, the real part of the transformation can be
specified exactly from the symmetrized record. Using the modulus of the

total transform together with the real part of the transform, one can infer the phase to within a sign. Thus a pair of images is derived, one erect, the other inverted. This ambiguity can be resolved, however, by translating the source in a known direction off axis.

The results derived for the spatial detection of intensity fluctuations are shown to be similar to previous results dealing with the phenomenon of laser speckle in terms of the spatial transform relations. However, the criterion of detector time resolution, central to the results of intensity interferometry, is absent for laser speckle effects. Thus, it can be inferred that the utility of intensity interferometry is based on the detection of a time-variant speckle pattern.

Finally, experimental evidence is offered to support the spatial transform relations predicted here. In addition, a time-domain intensity-correlation experiment is performed, the purpose of which is to infer the existence of a time-varying speckle pattern.

TABLE OF CONTENTS

TABLE OF CONTENTS (CONT.)

Page

6

LIST OF ILLUSTRATIONS

7

PREFACE

The history of intensity interferometry is rooted in the work of
Hanbury Brown and Twiss. Their earliest investigations[1]* dealt with the
problem of resolving stellar radio sources by a technique involving the
correlation of the squared outputs of two receivers. The advantages are
the reduction of certain kinds of experimental constraints as well as
the comparative insensitivity of the method to atmospheric scintillation.[2]
A preliminary conclusion reached at that time was that this technique of
intensity correlation would not be applicable at optical frequencies
because of limitations imposed by photon noise. However, in later work,[3]
Hanbury Brown and Twiss showed that meaningful intensity correlations
could be made at optical frequencies even with highly degenerate sources.
The limitations placed on this approach by quantum noise and detector
efficiency have been severe, calling for highly refined experimental
technique.

For laser illumination, the situation is very different. The signal-
to-noise ratio can be typically increased by six orders of magnitude.[4]
However, the statistics of the source must be considered in the measure-
ment. The key to relating intensity correlations to some property
involving field correlations lies in the assumption of gaussian statis-
tics,[5] for which all higher moments are determined from the first and
second. Single-mode lasers, though, are distinctly non-gaussian in their
temporal statistics and, therefore, cannot be described by theory framed
for thermal sources. But with the addition of axial modes. it has been
asserted[6] that the field amplitude becomes nearly gaussian distributed.

The principal formula used by Hanbury Brown and Twiss [Ref. 3b,
Eq. (2.1)] to infer the diameter of a distant source shows that the time-
averaged correlation of intensities at two points is equal to the product
of a function involving the temporal characteristics of the source with
the square of the spatial-Fourier transform of the source intensity dis-
tribution. Consideration of the source temporal statistics is necessary
if the intensity-product output of the detectors is averaged in the time
domain (as it nearly always is) to overcome the limitations imposed by
photon and detector noise and possibly reduce scintillation effects pro-
duced by transmission through the atmosphere. If the intent of an inten-
sity correlation experiment is to gain information concerning the source
intensity distribution, then the temporal statistics may be of little
interest in themselves.

Intensity interferometry can be understood as a two-point correlation
of intensities following the squaring of the electric field at the
detector. If the source is quasi-monochromatic, each differential ele-
ment on the object emits a number of temporal modes that interfere with
each other at the detector. If the detector has sufficient bandwidth to

---

*References are listed on page 66.

9

Preceding page blank

detect the~~ beat frequencies, the amplitude and phase of the incoming intensity beats are utilized. What is sufficient depends on the bandwidth of the source. For a thermal source, most beat frequencies are too high to be resolved even with the megacycle response of the Hanbury Brown - Twiss apparatus. For a single-mode laser, all beat frequencies could be less than 100 Hz. It is commonly argued that, in these circumstances, t e random fluctuations of the temporal statistics from different points of the source cause the beat frequencies from each source point to add incoherently at the detector. The time-averaged intensity correlation is then proportional to the squared spatial Fourier transform of the source intensity. This approach gives essentially a squared version of the van Cittert-Zernike theorem.[7]

We wish to suggest that the requirement of surface roughness at the source (to assure spatial incoherence) is sufficient to guarantee the incoherent addition of beat frequencies at the intensity detectors. Thus, if temporal noise (photon noise, time-dependent detector noise) is largely absent in a local spatial sense, as might be the case with a multi-axial-mode laser with photographic detection, then the intensity information might be gathered during one resolution time of the detector over a plane section normal to the direction of light propagation. Any noise arising in the process would be spatial, and might be averaged out by taking a sufficiently large area of spatial correlation. The reduction of atmospheric spatial noise would be similar to a process known as aperture averaging.[8] Film-grain noise would be extremely well averaged by the relatively large area of averaging.

The relative insensitivity of intensity interferometry to turbulence can be shown[2] if the propagation medium is assumed to be dispersionless over the range of carrier frequencies. Because each temporal frequency sees the same refractive index, the differential (beat) frequencies remain unchanged. However, the spatial-Fourier-transform relation between the source and the far-field scales as the average frequency, not the beat frequency, and thus the resolution afforded by optical frequencies is maintained.

The idea of examining spatial beat frequencies of second-order correlation is, of course, not new. Many classical field-correlation interferometers, as well as holographic experiments, are built on this principle, involving a spatial or time lag between interfering beams of the same source. More difficult is the spatial recording of beats from two independent sources, as demonstrated by Magyar and Mandel.[9]

In this thesis, we examine the subject of intensity interferometry in the spatial domain. In Section 1, an introduction to this field is given, leading up to the results of Hanbury Brown and Twiss and the extension of their work by Gamo.[10] In Section 2, using as a basis a mathematical framework due to Marchand and Wolf,[11] we generalize the concept of the mut· l coherence function to time averaging of arbitrary

length. The fourth-order field correlation function in the far zone is then formed, revealing a Fourier transform relationship with the source irradiance.

In Section 3, a technique of symmetrizing the electric field before detection is developed as a way of inferring the phase of the source-intensity Fourier transform. With this additional information, the transform can be inverted to form the intensity distribution for sources of arbitrary symmetry. In the next section, comparisons are made between spatial intensity interferometry and the phenomenon of laser speckle. Finally in Section 5, some experiments involving spatial intensity correlation are described. Included is an investigation into the relationship between the average-value and time-varying speckle patterns.

1. AN INTRODUCTION TO INTENSITY INTERFEROMETRY

1.1 Introduction

Central to the framework of intensity interferometry are two kinds of relationships, each existing in distinct domains. The first, and the principal, of these relationships lies in the spatial domain, since we are here primarily interested in optical imaging by means of intensity correlations. Specifically, by some manipulation of the far-field intensity distribution of a source, we wish to infer the intensity distribution over the source itself. However, the efficacy of this intent rests almost totally on the constraints of a second area of relationships, the temporal domain. It is here that the bandwidth, power, and time stability of the carrier waves are determined and even the practicality of this special kind of imaging.

In this chapter, we intend to give a systematic introduction to intensity interferometry. In essence this technique is straightforward. The fundamental principles are revealed in the well-known mathematical techniques of correlation and Fourier transformation. First, we will establish the basic spatial relationships between source and far field for both the first- and second-order cases. Next, we will show the relationship between second- and fourth-order field statistics for a gaussian time variable. Finally, we will describe the work of Hanbury Brown and Twiss and the extension of their work by Gamo.

1.2 The Huygens-Fresnel Principle

We wish to examine here the relationship between the electric field on a section of plane normal to the direction of energy transport with the field in a plane section at some later time. Referring to Figure 1.1, we call $V(\xi,\eta)$ the electric field bounded by the aperture Σ in the ξ-η
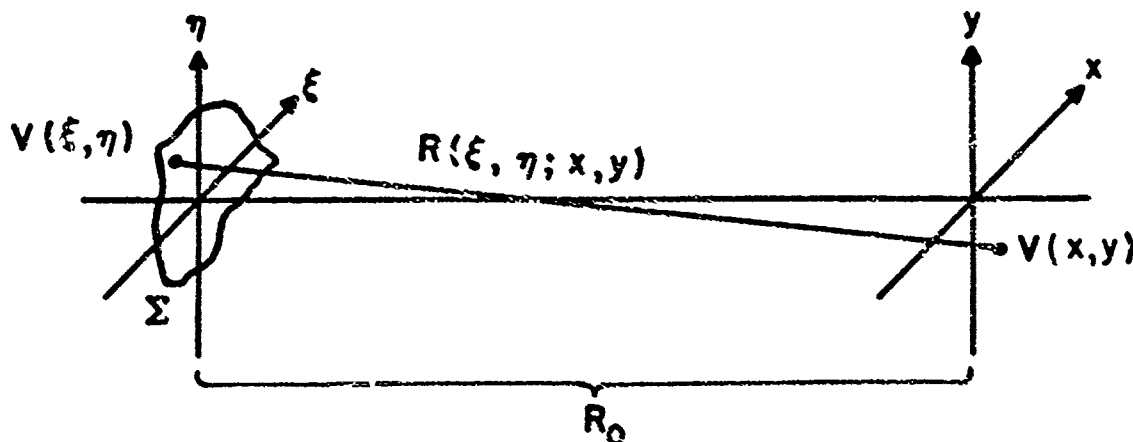
Figure 1.1   The Coordinate Axes for the Object (ξ-η) and Detection (x-y) Planes

13

plane. Upon realizing that each point in the aperture radiates a spherical wave to the right, we can directly write the Huygens-Fresnel principle (Ref. 7, Ch. 8) for paraxial waves for which

$$V(x,y;t) = \int\!\!\int_{-\infty}^{\infty} V(\xi,\eta;t) \frac{\exp[ikR(\xi,\eta;x,y)]}{i\lambda R(\xi,\eta;x,y)} d\xi d\eta, \qquad (1.1)$$

where $k = 2\pi/\lambda$, and λ equals the wavelength of the radiation. Equation (1.1) states that the electric field $V(x,y;t)$ is formed of a superposition of waves emanating from each point within the aperture, properly phase-shifted according to the exponential term and diluted by the $1/R$ expression. Now

$$R(\xi,\eta;x,y) = [R_o^2 + (x-\xi)^2 + (y-\eta)^2]^{\frac{1}{2}} \qquad (1.2a)$$

$$= R_o\left\{1 + \frac{1}{2}\left(\frac{x-\xi}{R_o}\right)^2 + \frac{1}{2}\left(\frac{y-\eta}{R_o}\right)^2\right\}, \qquad (1.2b)$$

when approximated by the first two terms of the binomial (the Fresnel approximation) expansion. Using Equation (1.2b) in Equation (1.1) and making the far-field (Fraunhofer) approximation $[R_o \gg k(\xi^2 + \eta^2)_{max}/2]$, we can write

$$V(x,y;t) = \frac{\exp[ik(R_o + (x^2+y^2)/2R_o)]}{i\lambda R_o}$$

$$\times \int\!\!\int_{-\infty}^{\infty} V(\xi,\eta;t)\exp\left[-i\frac{k}{R_o}(x\xi + y\eta)\right]d\xi d\eta. \qquad (1.3)$$

Apart from the coefficients before the integral, Equation (1.3) shows that the electric fields in an aperture and the far field are related by a spatial Fourier transform operation. This property is basic to the ensuing work involving intensity correlations with quasimonochromatic light.

1.3 The van Cittert-Zernike Theorem

Although Equation (1.3) holds for radiation of general frequencies, the relationship it expresses is somewhat academic here from the standpoint that it describes electric-field quantities that are unmeasurable

14

at optical wavelengths. It is this constraint that has prompted many investigators to couch optical theory in the form of correlations of field quantities. The most well known of these correlations is called the mutual coherence function, $\Gamma(\underline{x}_1, \underline{x}_2, \tau)$, where

$$\Gamma(\underline{x}_1, \underline{x}_2, \tau) \equiv \lim_{T \to \infty} \frac{1}{2T} \int_{-T}^{T} V(\underline{x}_1, t + \tau) V^*(\underline{x}_2, t) dt, \tag{1.4a}$$

$$= \overline{V(\underline{x}_1, t + \tau) V^*(\underline{x}_2, t)}, \tag{1.4b}$$

and τ is the time delay between the instantaneous product of the electric fields at the points $\underline{x}_1$ and $\underline{x}_2$. A special case of the mutual coherence function results when the time delay is set to zero or

$$\Gamma(\underline{x}_1, \underline{x}_2, \tau)_{\tau=0} \equiv J(\underline{x}_1, \underline{x}_2), \tag{1.5}$$

where $J(\underline{x}_1, \underline{x}_2)$ is called the mutual intensity function.

We wish to calculate the mutual intensity in the far field of a spatially incoherent source. Using Equations (1.5), (1.4b), and (1.3), we write

$$\overline{V(x_1, y_1; t) V^*(x_2, y_2; t)} = J(x_1, y_1; x_2, y_2) \tag{1.6a}$$

$$= \frac{\exp\left[\frac{i\overline{k}}{2R_0} (x_1^2 - x_2^2 + y_1^2 - y_2^2)\right]}{(\overline{\lambda R_0})^2} \iiiint_{-\infty}^{\infty} \overline{V(\xi_1, \eta_1; t) V^*(\xi_2, \eta_2; t)} \tag{1.6b}$$

$$\times \exp\left[-i \frac{\overline{k}}{R_0} (x_1 \xi_1 - x_2 \xi_2 + y_1 \eta_1 - y_2 \eta_2)\right] d\xi_1 d\xi_2 d\eta_1 d\eta_2,$$

where the processes of temporal averaging and spatial integration have been interchanged and the radiation assumed quasimonochromatic ($\nu_{min} \gg \nu_{max} - \nu_{min}$) so that the wavelength dependence can be approximated by the mean wavelength. Since the source is spatially incoherent, the mutual intensity takes the form[12]

$$\overline{V(\xi_1, \eta_1; t) V^*(\xi_2, \eta_2; t)} = J(\xi_1, \eta_1; \xi_2, \eta_2), \tag{1.7a}$$

$$= I(\xi, \eta) \delta(\xi_1 - \xi_2) \delta(\eta_1 - \eta_2). \tag{1.7b}$$

15

Physically, Equation (1.7b) implies that the time fluctuations of the electric fields at two non-identical points in the source plane are completely uncorrelated; equivalently, the total power measured at a point in the far field is simply the sum of the squared electric fields from each differential element of the source, taken with the proper phase delay and attenuation.

Using Equation (1.7b) in Equation (1.6), the mutual intensity collapses to a single area integral giving

$$J(x_1,y_1;x_2,y_2) = \frac{\exp\left[i\,\frac{\bar{k}}{2R_0}\,(x_1^2 - x_2^2 + y_1^2 - y_2^2)\right]}{(\bar{\lambda}R_0)^2}$$

$$\times \iint_{-\infty}^{\infty} I(\xi,\eta)\exp\left\{-i\,\frac{\bar{k}}{R_0}\,[(x_1 - x_2)\xi + (y_1 - y_2)\eta]\right\}d\xi d\eta. \qquad (1.8)$$

Although usually presented in a normalized form (Ref. 7, p. 510), Equation (1.8) is a statement of the van Cittert-Zernike theorem which, aside from the accompanying coefficient, shows that the mutual intensity in the far field of a spatially incoherent source is given by the Fourier transform of the intensity across that source. This theorem is basic to most optical imaging, since lenses effect the inverse transformation of Equation (1.8) to give a scaled distribution of the object irradiance. By the scaling property from one domain to another, intrinsic to the Fourier transform operation, large detail in the source is given by small separations in the far field and vice versa. Thus imaging with a finite aperture implies a finite limit to the high-frequency detail resolvable on the source. This justifies the well-known description of lenses as low-pass filters. Also, since there are many more pairs of points within an aperture corresponding to small separations than to large, there is a built-in redundancy weighted in favor of low-frequency resolution.

Equation (1.8), although a statement of second-order correlation, is basic also to fourth-order correlation, as we shall see later.

1.4 A Theorem Concerning the Fourth-Order Gaussian Random Process

We have just seen in Equation (1.7) the way in which a time average can be used to impose a condition on the correlation of an electric-field pair. No particular assumption was made about the statistics of the field variables. However, it is well known that classical thermal sources exhibit statistical fluctuations that are gaussian in nature. Hodara[6] has asserted that lasers with but a few axial modes are, to a good approximation, gaussian as well. However, Troup[13] has argued that gaussian statistics are achieved only in the limit of a large number of axial modes.

A well-known property of gaussian statistics is that all higher order moments are representable in terms of the first and second. A relation given by Middleton[14] reflecting this property gives the expectation value of the 2mth-order correlation for the zero-mean random variable $z_j = x_j - \bar{x}_j$, where

$$E(z_1 z_2 \ldots z_{2m}) = \sum_{\substack{\text{all} \\ \text{pairs}}} \left[\prod_{j \neq k}^{m} \overline{z_j z_k} \right],$$ (1.9a)

and
$$E(z_1 z_2 \ldots z_{2m+1}) = 0.$$ (1.9b)

We now use Equation (1.9a) to examine the relation between the fourth-order and lower-order moments of a complex-valued electric field variable that is gaussian in the domain in which the averaging takes place. We therefore write

$$E(I_1 I_2) = E(V_1 V_1^* V_2 V_2^*)$$ (1.10a)

$$= \overline{V_1 V_1^*} \, \overline{V_2 V_2^*} + \overline{V_1 V_2} \, \overline{V_1^* V_2^*} + \overline{V_1 V_2^*} \, \overline{V_1^* V_2}$$ (1.10b)

$$= \overline{I_1} \, \overline{I_2} + |\overline{V_1 V_2}|^2 + |\overline{V_1 V_2^*}|^2,$$ (1.10c)

where the complex conjugation has been used to assure a real expectation value. The first term of Equation (1.10c) is the product of the mean intensities at points one and two, while the last is the mutual coherence function defined by Equation (1.4a) if the overbars are taken as an average in the time domain and the ergodic hypothesis is assumed. We now examine the second term in this expression.

The electric field can be represented by the complex analytic signal[2] (where a constant term has been suppressed) as

$$V(t) = \int_0^\infty v(\omega) \exp(-i\omega t) d\omega,$$ (1.11)

where $v(\omega)$ exists only for positive frequencies. Using Equation (1.11), the second term of Equation (1.10c) can be expressed

17

$$\left| \overline{V_1(t)V_2(t)} \right|^2 =$$

$$\lim_{T \to \infty} \left| \frac{1}{2T} \int_{-T}^{T} \iint_{0}^{\infty} v_1(\omega_1) v_2(\omega_2) \exp[-i(\omega_1 + \omega_2)t] d\omega_1 d\omega_2 dt \right|^2, \quad (1.12a)$$

$$= \lim_{T \to \infty} \left| \iint_{0}^{\infty} v_1(\omega_1) v_2(\omega_2) \text{sinc}[(\omega_1 + \omega_2)T] d\omega_1 d\omega_2 \right|^2, \quad (1.12b)$$

where in going from Equation (1.12a) to (1.12b) the order of time and frequency integrations has been reversed, and sinc $x \equiv \sin x / x$. As the limit of T is taken, the sinc function approaches a delta function such that the integral has value only for $\pm\omega_1 = \mp\omega_2$. Since $v(\omega)$ can exist only for positive frequencies, the integral is zero.

Thus the fourth-order correlation of electric fields (second-order correlation intensities) given in Equation (1.10a) becomes

$$\overline{I_1 I_2} = \overline{I_1}\, \overline{I_2} + \left| \Gamma_{12} \right|^2, \quad (1.13)$$

where the defining relation of Equation (1.4a) has been used.

Equation (1.13), therefore, describes the relationship between the intensity and the field correlations for a process that is gaussian in the time domain. We note that, in general, the field correlation is a complex quantity, so that only the relationship between the intensity correlation and the modulus of the field correlation is implied. It reveals the underlying principle by which intensity correlations in the far field may be used to infer the accompanying field correlations and hence, through Equation (1.8), to gain knowledge of the intensity distribution at the source.

1.5 Intensity Interferometry in the Temporal Domain

As indicated initially in the Preface, Hanbury Brown and Twiss[1] were the first to realize the potential of using intensity beats to derive information concerning the irradiance of a distant source. First working at radio frequencies and then later at optical wavelengths,[3] Hanbury Brown and Twiss formulated the imaging problem and used the results to infer the diameter of the star Sirius. We wish to present a brief outline of their work which relates to the problem at hand.

Following Reference 3b, Hanbury Brown and Twiss express the electric field as a superposition of quasimonochromatic waves emitted from a differential area in the form

$$V(\underline{x}) \propto \sum_{r=0}^{\infty} h_r(\underline{\xi}) \cos\left[\frac{2\pi r}{T}\left\{t - \frac{R(\underline{\xi},\underline{x})}{c}\right\} - \chi_r(\underline{\xi})\right], \qquad (1.14)$$

where $h_r^2(\underline{\xi})d\underline{\xi}$ is proportional to the population of the rth mode, c is the vacuum velocity of light, T is the time of observation, and $\chi_r(\underline{\xi})$ is a random phase that is uniformly distributed between 0 and 2π radians. This phase is both time and space dependent. The condition of spatial incoherence, expressed earlier in the form of Equation (1.7), was assured by Hanbury Brown and Twiss by requiring that

$$\chi_r(\underline{\xi})\chi_s(\underline{\xi}') = \delta_{rs}\delta(\underline{\xi} - \underline{\xi}'). \qquad (1.15)$$

Using Equation (1.14), the instantaneous intensity is formed, where

$$I(\underline{x},t) \propto \iint_{-\infty}^{\infty} d\underline{\xi}d\underline{\xi}' \sum_{r>s} \sum_{s=1}^{\infty} \int_{-\infty}^{\infty} d\underline{x}\, \frac{2e(\alpha_{1r}\alpha_{1s}n_{1r}n_{1s})^{\frac{1}{2}}}{T}$$

$$\times \cos\left[\frac{2\pi(r-s)t}{T} - \frac{2\pi}{cT}\left\{rR(\underline{\xi},\underline{x}) - sR(\underline{\xi}',\underline{x})\right\} - \left\{\chi_r(\underline{\xi}) - \chi_s(\underline{\xi}')\right\}\right], \qquad (1.16)$$

n_{1r} is proportional to the number of quanta per mode, α_{1r} is the detector quantum efficiency, and e is the electronic charge; also, following Hanbury Brown and Twiss, two-dimensional spatial integration is indicated by single integral signs. In arriving at Equation (1.16), the form of Equation (1.14) was squared, giving a sum of two cosine terms, one involving a sum frequency, the other a difference frequency. The former term has been dropped, since it corresponds to a very high frequency term (approximately twice the mean optical frequency). The second term can be visualized in the form of a square $s \times r$ symmetrical matrix. The diagonal (r=s) corresponds to a dc term that has also been dropped, since the ensuing electronic apparatus has zero dc response. Twice the sum is taken of the off-diagonal terms in the upper half of the matrix.

Next, to account for the temporal resolution of the apparatus, the complex frequency response is represented by $F\left(\frac{r-s}{T}\right)$ so that the filtered current $J(\underline{x},t)$ is written

$$J(\underline{x},t) \approx \iint\limits_{-\infty}^{\infty} d\underline{\xi}d\underline{\xi}' \sum_{r>s}' \sum_{s=1} \int\limits_{-\infty}^{\infty} d\underline{x} \; \frac{2e(\alpha_{1r}\alpha_{1s}n_{1r}n_{1s})^{\frac{1}{4}}}{T}$$

$$\times \; \mathrm{Re}\left[F_{1}\left(\frac{r-s}{T}\right) \exp\left\{ i\left[\frac{2\pi}{T}\left\{ (r-s)t - \frac{rR(\underline{\xi},\underline{x}) - sR(\underline{\xi}',\underline{x})}{c} \right\} \right.\right.\right.$$

$$\left.\left.\left. - \left\{ \chi_{r}(\underline{\xi}) - \gamma_{s}(\underline{\xi}') \right\} \right] \right\} \right] . \qquad (1.17)$$

Invoking the Fresnel approximation [Equation (1.2b)] for the ray paths $R(\underline{\xi},\underline{x})$, Equation (1.17) is used to form the time-average cross-correlation function

$$C(\underline{f}') = \lim_{T_0 \to \infty} \frac{1}{T_0} \int_{0}^{T_0} J(\underline{x}_1, t - t_0)J(\underline{x}_2, t)dt, \qquad (1.18)$$

where

$$t_0 = \underline{k} \; (\underline{x}_1 - \underline{x}_2), \qquad f' = \underline{x} - \underline{x}', \qquad (1.19)$$

and $\underline{k}$ is a special kind of vector wave number defined by Hanbury Brown and $\overline{T}$wiss having dimensions of time/length. Under the assumption of ergodicity, the average defined by Equation (1.18) is taken as the equivalent of the ensemble average.

When Equation (1.17) is used to form the product of Equation (1.18), a pair of cosine terms result, similar to the step from Equation (1.14) to Equation (1.16). The first cosine argument involves a sum of phase terms, the second a difference. Reflecting on the condition expressed by Equation (1.15), it becomes apparent that only cosine terms independent of the random phases can contribute to the integral expressed by Equation (1.18). The cosine composed of sum terms therefore drops out, leaving the latter term with the additional constraint of Equation (1.15) forcing an equivalence among pairs of frequency variables, similar to the earlier result expressed by Equation (1.7).

The result of the operation defined by Equation (1.18) is

20

$$\overline{C(\underline{\xi}')} = 2e^2 \iiiint d\underline{\xi}d\underline{\xi}' \ d\underline{x}d\underline{x}' \int_0^\infty d\nu \alpha_1(\nu)\alpha_2(\nu)$$

$$\times \ [n_1(\nu,\underline{\xi})n_2(\nu_1,\underline{\xi})n_1(\nu,\underline{\xi}')n_2(\nu,\underline{\xi}')]^{\frac{1}{2}} \qquad (1.20)$$

$$\times \ \cos\left\{\frac{2\nu}{cR_0}(\underline{x}-\underline{x}')(\underline{\xi}-\underline{\xi}')\right\} \int_0^\infty \frac{df}{2}\left\{F_1(f)F_2^*(f) + F_1^*(f)F_2(f)\right\} ,$$

a relationship that can more succinctly be expressed in the form

$$\overline{C(\underline{\xi}')} = |\Gamma(\overline{\nu},\underline{\xi}')|^2 \ \overline{C(0)} , \qquad (1.21)$$

where

$$|\Gamma(\overline{\nu},\underline{\xi}')|^2 = \frac{\iint_{-\infty}^{\infty} d\underline{\xi}d\underline{\xi}' \ I(\underline{\xi})I(\underline{\xi}') \ \cos\left\{\frac{2\pi\overline{\nu}}{cR_0}\underline{\xi}' \cdot (\underline{\xi}-\underline{\xi}')\right\}}{\iint_{-\infty}^{\infty} d\underline{\xi}d\underline{\xi}' \ I(\underline{\xi})I(\underline{\xi}')} , \qquad (1.22)$$

and $\overline{C(0)}$ is the correlation at zero spacing of the two intensity detectors. Equation (1.21) is the principal result, revealing a particularly important relationship. It is shown that the process of intensity correlation in the far field with an infinite time average can be formulated as a product of two distinct terms. The first involves the square of the Fourier transform of the irradiance distribution across the source. The second term assumes the role of proportionality constant and relates to the power of the beat-frequency carrier.

We note that the source spatial information and coefficient term, $\overline{C(0)}$, are completely decoupled for the above condition of temporal averaging. This important result leads us to speculate under what conditions an illuminated rough surface might enjoy a similar description of decoupled space-time statistics for the case in which short time averaging takes place. In Section 2. this subject will be explored.

Finally, we see that Equation (1.22) gives the squared modulus of the spatial Fourier transform of the source distribution. This means that, unfortunately, except for certain situations for which the phase of the transform is known *a priori*, Equation (1.22) cannot be inverted to find $I(\underline{\xi})$. A method to circumvent this constraint is the subject of the next section.

1.6 The Triple Correlator of Gamo

As we have found in the two previous sections, fourth-order field correlation yields information only about the absolute square of the second-order correlation. Equivalently, only a power-spectral measurement is made relating to a function that is, in general, complex. Thus it is impossible to invert the power spectrum to derive the far-field mutual-intensity function and thence the irradiance distribution over a spatially incoherent surface.

In order to gain information about the phase of the mutual coherence function by the method of intensity correlations, Gamo[10] proposed a sixth-order correlation technique. We discuss briefly the principle. Using Equations (1.9a) and (1.4a), the third-order correlation of intensities becomes

$$E(I_1 I_2 I_3) = E(V_1 V_1^* V_2 V_2^* V_3 V_3^*) \tag{1.23a}$$

$$= \bar{I}^3 + \bar{I} (|\Gamma_{12}|^2 + |\Gamma_{23}|^2 + |\Gamma_{31}|^2) $$

$$+ 2|\Gamma_{12}| |\Gamma_{23}| |\Gamma_{31}| \cos(\phi_{12} + \phi_{23} + \phi_{31}), \tag{1.23b}$$

where $\bar{I}_1 = \bar{I}_2 = \bar{I}_3 = \bar{I}$, and the terms in ϕ_{ij} indicate the phase difference between points i and j. Using the identity

$$\overline{\Delta I_1 \Delta I_2 \Delta I_3} = \overline{I_1 I_2 I_3} - \bar{I}^3 - \bar{I}(|\Gamma_{12}|^2 + |\Gamma_{23}|^2 + |\Gamma_{31}|^2), \tag{1.24}$$

where $\Delta I_j = I_j - \bar{I}_j$, Equation (1.23b) can be used to write

$$\overline{\Delta I_1 \Delta I_2 \Delta I_3} = 2|\Gamma_{12}| |\Gamma_{23}| |\Gamma_{31}| \cos(\phi_{12} + \phi_{23} + \phi_{31}). \tag{1.25}$$

It can be seen from Equation (1.25) that the argument of the cosine function involves the sums of phase differences between the three sampling points. Gamo used the argument of the cosine to form a difference equation through which he expressed the phase of the two-point mutual coherence function. An ambiguity arises, however, in the sign of the phase because of the sign indeterminacy of the cosine argument. In effect, two images are derived, one the reflection through the origin of the other, and supplementary information must be used to resolve the proper reconstruction.

22

1.7 Summary

We have seen that, using the basic Huygens-Fresnel imaging equation, the fundamental observable of optical radiation, the intensity, can be used by means of the van Cittert - Zernike equation, to infer the distribution of intensity over a spatially incoherent source. Further, by means of the moment reduction formula of gaussian statistics, we have shown how higher-order moments can be used to infer certain properties of the second moment, the mutual coherence function. This property, for the fourth-order moment, is inherent to the Hanbury Brown - Twiss formulation. Finally, we have seen the general way in which Gamo used the technique of sixth-order field correlation to derive the phase of the second-order field correlation.

This introduction will serve as a basis upon which we will extend the principle of intensity interferometry to detection and averaging in the spatial domain.

2. INTENSITY INTERFEROMETRY IN THE SPATIAL DOMAIN

2.1 Introduction

In this section, we will examine the problem of using intensity measurements in the far field to infer the irradiance distribution over a rough surface. However, rather than examining the two-point, time-averaged correlation of intensities, the far-field intensity pattern will be recorded for one time-resolution unit of the detector. The spatial signal will then be autocorrelated and related to the irradiance.

We start with a straightforward generalization of a method given recently by Marchand and Wolf.[11] Our notation is similar and we follow closely their development through their Equation (35).

2.2 The Intermediate-Average Mutual Coherence Function

For a stationary scalar wave field, the mutual coherence function for the correlation of two space-time points is often written

$$\Gamma(\underline{x}_1, \underline{x}_2, \tau, T) \equiv \frac{1}{2T} \int_{-T}^{T} V_T(\underline{x}_1, t + \tau) V_T^*(\underline{x}_2, t) dt, \qquad (2.1)$$

where $\underline{x}_n = x_n \hat{i} + y_n \hat{j}$, and the limits for the time integration are allowed to approach infinity. For this case, however, we wish to keep the parameter T finite and by the subscripts indicate that we assume a knowledge of $V_T(\underline{x}_1, t + \tau)$ and $V_T^*(\underline{x}_2, t)$ only over the finite sample length

$2T$. We wish to call $\Gamma(\underline{x}_1, \underline{x}_2, \tau, T)$ the intermediate-average mutual

23

coherence function and carefully stress that, for arbitrary T or shift of origin, it may bear little resemblance to the mutual coherence function defined by the ensemble average.

Following Reference 11, we represent $V(\underline{x},t)$ as the temporal Fourier transform of the complex analytic signal (where a constant term $(2\pi)^{-1}$ is suppressed)

$$V_T(\underline{x},t) = \int_0^\infty v_T(\underline{x},\omega) \exp(-i\omega t)d\omega, \quad \text{for} \quad 0 \leq |t| \leq T \quad (2.2a)$$

$$= 0 \quad \text{otherwise}, \quad (2.2b)$$

and

$$v_T(\underline{x},\omega) = \int_{-T}^T V_T(\underline{x},t) \exp(i\omega t)dt. \quad (2.2c)$$

Substituting Equation (2.2a) into Equation (2.1), interchanging the order of integration, and time-averaging and performing the time integration, we get

$$\Gamma(\underline{x}_1,\underline{x}_2,\tau,T) = \iint_0^\infty W_T(\underline{x}_1,\underline{x}_2,\omega_1,\omega_2) \exp(-i\omega_1\tau)\text{sinc}[(\omega_1 - \omega_2)T]d\omega_1 d\omega_2,$$

$$(2.3)$$

where

$$\text{sinc } x \equiv \frac{\sin x}{x}, \quad (2.4)$$

and the cross-spectral density function

$$W_T(\underline{x}_1,\underline{x}_2,\omega_1,\omega_2) \equiv v_T(\underline{x}_1,\omega_1)v_T^*(\underline{x}_2,\omega_2), \quad (2.5)$$

and the subscript T here and later implies a function based on the electric field statistics only for the particular sample 2T in length (hereafter called the detector resolution time) about the origin. The sinc function of Equation (2.3) assumes the role of a low-pass filter. If T is very small, the two frequency variables of Equation (2.3) are essentially independent and all cross terms are represented in the product of Equation (2.5). These cross terms form a high-frequency spectral content. However, as T tends to infinity, the sinc function assumes the role of a delta function, constraining correlation to occur only between identical frequencies in the transform product and forcing the integral to a one-dimensional form. In the limit of large T, the filtered spectrum of Equation (2.5) becomes the mean square value (dc) of each temporal frequency component in the signal.

24

Following Marchand and Wolf[11] and the earlier lead of Walther,[15] $v_T(\underline{x},\omega)$ is represented in the form of an angular (spatial) spectrum of plane waves in Cartesian coordinates where

$$v_T(\underline{x},\omega) = \iint\limits_{-\infty}^{\infty} a_T(p,q,\omega) \exp[ik(px + qy + mz)]dpdq, \qquad (2.6)$$

$$m = (1 - p^2 - q^2)^{\frac{1}{2}} \quad \text{if } p^2 + q^2 \leq 1 \qquad (2.7a)$$

$$= i(p^2 + q^2 - 1)^{\frac{1}{2}} \quad \text{if } p^2 + q^2 > 1, \qquad (2.7b)$$

and

$$k = \omega/c, \qquad (2.8)$$

where c is the vacuum velocity of light. Equation (2.6) indicates that $v_T(\underline{x},\omega)$ is formed by a superposition of homogeneous spatial waves propagating in the half space $z > 0$ for the criterion expressed by Equation (2.7a) and a set of evanescent waves propagating parallel to the plane $z = 0$ for the case described by Equation (2.7b).

Expressing Equation (2.5) in the form of the angular spectrum of plane waves defined by Equation (2.6), we get

$$W_T(\underline{x}_1,\underline{x}_2,\omega_1,\omega_2) = \iiiint\limits_{-\infty}^{\infty} A_T(p_1,q_1;p_2,q_2;\omega_1,\omega_2)$$

$$\times \exp[ik_1(p_1x_1 + q_1y_1 + m_1z_1)] \qquad (2.9)$$

$$\times \exp[-ik_2(p_2x_2 + q_2y_2 + m_2z_2)]dp_1dq_1dp_2dq_2,$$

where

$$A_T(p_1,q_1;p_2,q_2;\omega_1,\omega_2) \equiv a_T(p_1,q_1;\omega_1)a_T^*(p_2,q_2;\omega_2). \qquad (2.10)$$

Using Equation (2.9), therefore, the intermediate-average mutual coherence function of Equation (2.3) can be written

25

$$\Gamma(\underline{x}_1,\underline{x}_2,\tau,T) = \int\!\!\!\int_0^\infty \exp(-i\omega_1\tau)\ \mathrm{sinc}[(\omega_1 - \omega_2)T]d\omega_1 d\omega_2$$

$$\times\ \int\!\!\!\int\!\!\!\int\!\!\!\int_{-\infty}^\infty A_T(p_1,q_1;p_2,q_2;\omega_1,\omega_2)$$

(2.11)

$$\times\ \exp[ik_1(p_1x_1 + q_1y_1 + m_1z_1)]$$

$$\times\ \exp[-ik_2(p_2x_2 + q_2y_2 + m_2z_2)]dp_2dq_2dp_2dq_2.$$

If T is allowed to approach infinity, the limiting form of the sinc function forces $\omega_1 = \omega_2$, and the intermediate-average mutual coherence function clearly reduces to the form of Equation (2.13) of Reference 11 by the elimination of one of the time-frequency integrals.

2.3 The Angular Correlation Function and Other Spatial Correlation Functions

The cross-spectral density function $W_T(\underline{x}_1,\underline{x}_2;\omega_1,\omega_2)$ is now expressed as a four-dimensional spatial Fourier integral as

$$W_T(x_1,y_1,z_1;x_2,y_2,z_2;\omega_1,\omega_2) = \int\!\!\!\int\!\!\!\int\!\!\!\int_{-\infty}^\infty \hat{W}_T(f_1,g_1;z_1;f_2,g_2;z_2;\omega_1,\omega_2)$$

$$\times\ \exp[i(f_1x_1 + g_1y_1 + f_2x_2 + g_2y_2)]df_1dg_1df_2dg_2. \qquad (2.12)$$

Equation (2.9) with Equation (2.12) therefore implies

$$A_T(p_1,q_1;p_2,q_2;\omega_1,\omega_2) = k_1^2k_2^2\hat{W}_T(k_1p_1,k_1q_1;z_1;-k_2p_2,-k_2q_2;z_2;\omega_1,\omega_2)$$

$$\times\ \exp[-i(k_1m_1z_1 - k_2m_2z_2)], \qquad (2.13)$$

and specifically if $z_1 = z_2 = 0$, Equation (2.13) becomes

$$A_T(p_1,q_1;p_2,q_2;\omega_1,\omega_2) = k_1^2k_2^2\hat{W}_T(k_1p_1,k_1q_1;0;-k_2p_2,-k_2q_2;0;\omega_1,\omega_2).$$

(2.14)

Equation (2.14) indicates that the angular correlation function

$A_T(p_1, q_1; p_2, q_2; \omega_1, \omega_2)$ and the four-dimensional spatial Fourier transform of the cross-spectral density function are related at the plane $z = 0$ if $f_1 = k_1 p_1$, $g_1 = k_1 q_1$, $f_2 = -k_2 p_2$, and $g_2 = -k_2 q_2$.

Further, the spatial transform of the time spectrum of the field can be represented by

$$v_T(x, y, z; \omega) = \iint\limits_{-\infty}^{\infty} \hat{v}_T(f, g; z; \omega) \, \exp[i(fx + gy)] df dg. \qquad (2.15)$$

Comparison of Equations (2.15) and (2.6) indicates

$$a_T(p, q; \omega) = k^2 \hat{v}_T(kp, kq, z, \omega) \, \exp(-ikmz). \qquad (2.16)$$

Using Equation (2.16) in Equation (2.1) gives

$$A_T(p_1, q_1; p_2, q_2; \omega_1, \omega_2) = k_1^2 k_2^2 \hat{v}_T(k_1 p_1, k_1 q_1, z_1; \omega_1)$$

$$\times \quad \hat{v}_T^*(k_2 p_2, k_2 q_2, z_2; \omega_2) \qquad (2.17)$$

$$\times \quad \exp[-i(k_1 m_1 z_1 - k_2 m_2 z_2)].$$

The intermediate-average spatial correlation function is defined

$$\hat{v}_T(k_1 p_1, k_1 q_1, z_1; \omega_1) \hat{v}_T^*(k_2 p_2, k_2 q_2, z_2; \omega_2)$$

$$\equiv V_T(k_1 p_1, k_1 q_1; z_1; k_2 p_2, k_2 q_2; z_2; \omega_1, \omega_2) \qquad (2.18a)$$

$$= V_T(k_1 p_1, k_1 q_1; 0; k_2 p_2, k_2 q_2; 0; \omega_1, \omega_2)$$

$$\times \quad \exp[i(k_1 m_1 z_1 - k_2 m_2 z_2)], \qquad (2.18b)$$

where the product form of Equation (2.18b) is implied by the independence of the left side of Equation (2.17) on z_1 and z_2. If we set $z_1 = z_2 = 0$, Equations (2.17) and (2.18) imply

$$A_T(p_1, q_1; p_2, q_2; \omega_1, \omega_1) = k_1^2 k_2^2 V_T(k_1 p_1, k_1 q_1; 0; k_2 p_2, k_2 q_2; 0; \omega_1, \omega_2). \qquad (2.19)$$

27

Finally, using Equations (2.14) and (2.19), we find

$$V_T(f_1,g_1;0;f_2,g_2;0;\omega_1,\omega_2) = \hat{W}_T(f_1,g_1;0;-f_2,-g_2;0;\omega_1;\omega_2). \qquad (2.20)$$

Thus the relationships between the angular correlation function and the cross-spectral density function are established by Equation (2.14) and the angular correlation function and the spatial frequency correlation function by Equation (2.19) for the case of intermediate time averaging.

2.4 The Intermediate-Average Correlation Function in the Far Field

Now the form of the cross-spectral density function is examined in the far field. Defining $r_n = (x_n{}^2 + y_n{}^2 + z_n{}^2)^{\frac{1}{2}}$, we seek the asymptotic forms for the case of $\underline{x}_1$ and $\underline{x}_2$ tending to infinity in the paths indicated by the direction cosines

$$\frac{x_2}{r_2}, \frac{y_2}{r_2}, \frac{z_2}{r_2} \quad \text{and} \quad \frac{x_1}{r_1}, \frac{y_1}{r_1}, \frac{z_1}{r_1}.$$

Rewriting Equation (2.9) using the definition of Equation (2.10), we have

$$W_T(\underline{x}_1,\underline{x}_2;\omega_1,\omega_2) = \iint\limits_{-\infty}^{\infty} a_T(p_1,q_1;\omega_1) \exp[ik_1(p_1x_1 + q_1y_1 + m_1z_1)]dp_1dq_1$$

$$\times \iint\limits_{-\infty}^{\infty} a_T^*(p_2,q_2;\omega_2) \exp[-ik_2(p_2x_2 + q_2y_2 + m_2z_2)]dp_2dq_2. \qquad (2.21)$$

As $k_1r_1 \to \infty$ and $k_2r_2 \to \infty$, the asymptotic form of the two-dimensional integrals is given by Miyamoto and Wolf[16] as

$$W_T(\underline{x}_1,\underline{x}_2;\omega_1,\omega_2) = \frac{(2\pi)^2}{k_1k_2} \cos\theta_1 \cos\theta_2 \, A_T\!\left(\frac{x_1}{r_1}, \frac{y_1}{r_1}; \frac{x_2}{r_2}, \frac{y_2}{r_2};\omega_1,\omega_2\right)$$

$$\times \frac{\exp[i(k_1r_1 - k_2r_2)]}{r_1r_2}, \qquad (2.22)$$

where

$$\frac{z_1}{r_1} \equiv \cos\theta_1, \quad \frac{z_2}{r_2} \equiv \cos\theta_2 \qquad (2.23)$$

28

and use of Equation (2.10) has been made. Finally, if Equation (2.22) is substituted into Equation (2.3), we get for the intermediate-average mutual coherence function

$$\Gamma(\underline{x}_1,\underline{x}_2,\tau,T) = \iint\limits_0^\infty \exp(-i\omega_1\tau) \; \text{sinc}\,[(\omega_1 - \omega_2)T]d\omega_1 d\omega_2$$

$$\times \quad \frac{4\pi^2}{k_1 k_2} \cos\,\theta_1\,\cos\,\theta_2 \;\frac{\exp[i(k_1 r_1 - k_2 r_2)]}{r_1 r_2} \qquad (2.24)$$

$$\times \quad A_T\!\left(\frac{x_1}{r_1},\,\frac{y_1}{r_1},\,\frac{x_2}{r_2},\,\frac{y_2}{r_2},\,\omega_1,\omega_2\right).$$

In addition, because of the relationship given earlier relating the angular correlation function to the cross-spectral density and the spatial-frequency functions [Equations (2.14) and (2.19)], Equation (2.22) can be written in the following forms:

$$W_T(\underline{x}_1,\underline{x}_2;\omega_1,\omega_2) \sim 4\pi^2\,\cos\,\theta_1\,\cos\,\theta_2\,k_1 k_2\;\frac{\exp[i(k_1 r_1 - k_2 r_2)]}{r_1 r_2}$$

$$\times \quad \hat{W}_T\!\left(\frac{k_1 x_1}{r_1},\,\frac{k_1 y_1}{r_1};\,0;\,-\frac{k_2 x_2}{r_2},\,-\frac{k_2 y_2}{r_2};\,0;\,\omega_1,\omega_2\right) \qquad (2.25a)$$

$$= \quad 4\pi^2\,\cos\,\theta_1\,\cos\,\theta_2\,k_1 k_2\;\frac{\exp[i(k_1 r_1 - k_2 r_2)]}{r_1 r_2}$$

$$\times \quad V_T\!\left(k_1\,\frac{x_1}{r_1},\,k_1\,\frac{y_1}{r_1};\,0;\,k_2\,\frac{x_2}{r_2},\,k_2\,\frac{y_2}{r_2};\,0;\,\omega_1,\omega_2\right). \qquad (2.25b)$$

Equations (2.25a) and (2.25b) can also be used in Equation (2.3) to provide alternate forms of Equation (2.24). Equations (2.24) and (2.25) form the modified version of the forms given in Reference 11, Equations (2.33) through (2.35). Using these results, we are now in a position to form the self-intensity function in the far field.

2.5 The Self-Intensity Function in the Far Field

We now examine the form of the self-intensity in the far field by letting points $\underline{x}_1 = \underline{x}_2 = \underline{x}$ and then letting the time delay, τ, be

zero. Under these conditions, the mutual coherence function reduces to the self-intensity (Reference 7, pp. 507-509) and, using Equation (2.25b) in Equation (2.3) and the definition given in Equation (2.18a), we have

$$
I(\underline{x},T) = 4\pi^2 \cos^2\theta \iint\limits_{0}^{\infty} d\omega_1 d\omega_2 \frac{\omega_1 \omega_2}{c} \frac{\exp[i(k_1 - k_2)r]}{r^2} \operatorname{sinc}\{(\omega_1 - \omega_2)T\}
$$

$$
\times \hat{v}_T\left(k_1 \frac{x}{r}, k_1 \frac{y}{r}; 0; \omega_1\right) \hat{v}_T^*\left(k_2 \frac{x}{r}, k_2 \frac{y}{r}; 0; \omega_2\right), \qquad (2.26)
$$

where, as indicated earlier, the sinc function acts to suppress temporal frequencies in the cross spectrum higher than $\sim 1/(2T)$ Hz. We now utilize the linear transformation of the time frequency variables (for which the jacobian is unity) defined by

$$
\omega_1 - \omega_2 \equiv \rho \quad \text{and} \quad \frac{\omega_1 + \omega_2}{2} \equiv \sigma. \qquad (2.27)
$$

Writing the ω variables in terms of these center-of-mass coordinates,

$$
\omega_1 = \frac{2\sigma + \rho}{2} \quad \text{and} \quad \omega_2 = \frac{2\sigma - \rho}{2}, \qquad (2.28)
$$

which, when substituted into Equation (2.26), gives

$$
I(\underline{x},T) = \left(\frac{2\pi}{cr}\right)^2 \cos^2\theta \int_{\sigma=0}^{\infty} d\sigma\, \sigma^2 \int_{\rho=-\infty}^{\infty} \operatorname{sinc}(\rho T)\exp(i\rho r/c)d\rho
$$

$$
\times \hat{v}_T\left(\frac{\sigma + \rho/2}{c} \frac{x}{r}, \frac{\sigma + \rho/2}{c} \frac{y}{r}; 0; \sigma + \rho/2\right) \qquad (2.29)
$$

$$
\times \hat{v}_T^*\left(\frac{\sigma - \rho/2}{c} \frac{x}{r}, \frac{\sigma - \rho/2}{c} \frac{y}{r}; 0; \sigma - \rho/2\right),
$$

where the dependence of the amplitude on the difference-frequency coordinate, ρ, has been dropped, since for quasimonochromatic radiation $\sigma^2 \gg |\rho^2/4|$.

Now, using the defining transform relation of Equation (2.15), we write the spatial correlation function at the source ($z=0$) where

$$\hat{v}_T\left(\frac{\sigma+\rho/2}{c}\frac{x}{r},\frac{\sigma+\rho/2}{c}\frac{y}{r};\;0;\;\sigma+\rho/2\right)\hat{v}_T^*\left(\frac{\sigma-\rho/2}{c}\frac{x}{r},\;\frac{\sigma-\rho/2}{c}\frac{y}{r};\;0;\;\sigma-\rho/2\right)$$

$$=\frac{1}{(2\pi)^2}\iiiint_{-\infty}^{\infty}v_T(\xi_1,\eta_1;0;\sigma+\rho/2)\;v_T^*(\xi_2,\eta_2;0;\sigma-\rho/2)\qquad(2.30)$$

$$\exp\left[-i\left(\frac{\sigma+\rho/2}{c}\right)\left(\xi_1\,\frac{x}{r}+\eta_1\,\frac{y}{r}\right)\right]\exp\left[i\left(\frac{\sigma-\rho/2}{c}\right)\left(\xi_2\,\frac{x}{r}+\eta_2\,\frac{y}{r}\right)\right]\,d\xi_1 d\xi_2 d\eta_1 d\eta_2.$$

Now the intermediate-average spatial-correlation function,

$$v_T(\xi_1,\eta_1;\;0;\;\sigma+\rho/2)\;v_T^*(\xi_2,\eta_2;\;0;\;\sigma-\rho/2),$$

when considered with the filtering action of the sinc function of Equation (2.29) will have an effective contribution only for the low-frequency components formed by the difference-frequency terms $\sim 1/(2T)$ Hz or less.

In addition, we assume the mode population to be a slowly varying function of σ, since $\sigma \gg \rho/2$. This approximation can be couched mathematically by expressing the mode population in a Taylor-series expansion about some center frequency σ_c and taking only the first (constant) term. This gives the idealized mode population the shape of a rectangle function. Thus we write

$$[v_T(\xi_1,\eta_1,0;\sigma+\rho/2)\;v_T^*(\xi_2,\eta_2,0;\sigma-\rho/2)]_{\text{low freq.}}$$

$$= A(\xi_1,\eta_1;\sigma+\rho/2)\;A(\xi_2,\eta_2;\sigma-\rho/2)\;\exp[i\phi(\xi_1-\xi_2,\eta_1-\eta_2;\rho)]\quad(2.31a)$$

$$= A(\underline{\xi}_1,\sigma)\;A(\underline{\xi}_2,\sigma)\;H(\rho)\;\exp[i\phi(\underline{\xi}_1-\underline{\xi}_2;\rho)],\qquad(2.31b)$$

where

$$H(\rho)=\begin{cases}1 & \text{for } A(\underline{\xi};\;\sigma\pm\rho/2)\neq 0 \\[2mm] 0 & \text{otherwise.}\end{cases}$$

Equation (2.31) acknowledges the loss of the optical-frequency phase, while maintaining the phase of the intensity envelope formed by temporal beat modes. The degree to which the phase of this envelope is detected depends on the bandwidth of the source and the detector resolution, 2T.

31

Essentially, these arguments were made by Hanbury Brown and Twiss
(Reference 3b, p. 311), except for the defining of the H function. Its
introduction is brought about by the description of narrow-band sources
by terms in $A(\xi,\sigma)$. For a thermal source of relatively large bandwidth,
the maximum difference ρ will extend far beyond the temporal-frequency
response of the system [here reflected in the sinc term of Equation (2.24)]
and be continuous as well. But for a laser source exhibiting a series of
axial modes, the complete difference-frequency domain might lie entirely
within the system response but be piece-wise continuous in its extent.

Relative to the representation of the intermediate-average by the
form of Equation (2.31), we wish to reiterate a statement made following
Equation (2.1) that the intermediate-averaging process may bear little
resemblance to the infinite time average, even so far as the detail of
the amplitude terms, $A(\xi,\sigma)$. This situation would be serious if our
intent were to infer, for example, the time-frequency statistics of the
source. but in the present concept, we desire only to infer the spatial
properties of the source. If we consider a multi-axial-mode laser beam
scattered from a spatially rough surface, the lack of correspondence
between the two averages is unimportant, for all such mode history is
integrated out; all areas of the scatterer see the same mode characteris-
tics. Any mode fluctuation would be seen simply as a variation in
total received power from one sample to the next. Here, we simply
require for one detector-resolution time over a spatial domain that the
process of Equation (2.31) maintain the random phase term $\phi(\underline{\xi}_1 - \underline{\xi}_2, \rho)$
(due either to the temporal mode structure of the source or to the scat-
tering surface roughness) with sufficient mode population [reflected in
the amplitude terms $A(\underline{\xi},\sigma)$] such that quantum noise in both the carrier
wave and the detector can be ignored.

Using the results of Equation (2.31) in Equation (2.29) and taking
$\theta \ll 1$, we write

$$I(P,T) = \left(\frac{1}{cr}\right)^2 \int_0^\infty c^2 \, d\sigma \int_{-\infty}^\infty d\rho \, \exp(i\rho r/c) \, \text{sinc}(\rho T) H(\rho)$$

$$\times \iiiint_{-\infty}^\infty A(\underline{\xi}_1,\sigma) \, A(\underline{\xi}_2,\sigma) \, \exp[i\phi(\underline{\xi}_1 - \underline{\xi}_2; \rho)] \tag{2.32}$$

$$\times \exp\left[-i\left(\frac{\sigma + \rho/2}{c}\right)\left(\xi_1 \frac{x}{r} + \eta_1 \frac{y}{r}\right)\right] \exp\left[i\left(\frac{\sigma - \rho/2}{c}\right)\left(\xi_2 \frac{x}{r} + \eta_2 \frac{y}{r}\right)\right] d\xi_1 d\xi_2 d\eta_1 d\eta_2.$$

We now have the self-intensity in the far field expressed as a double
integral over sum- and difference-frequency components as well as two,
two-dimensional spatial Fourier transforms over the source.

32

Following Goodman,[17] we argue that the received field at any point in the far zone consists of a sum of random-amplitude, random-phase, complex phasors contributed by the elementary scatterers. If the size of the scattering area is large enough to include many point scatterers (or there are enough elementary coherence areas composing the source), the Central Limit Theorem may be used to conclude that the electric field in the detection plane is a gaussian random process in a spatial sense.

Using the form of Equation (2.32) and its property of spatial gaussian statistics, we are ready to form the fourth-order correlation function in the far zone.

2.6 Fourth-Order Field Correlation in the Far Zone

In Section 1.4, a theorem of fourth-order gaussian processes was derived. This relation is implicit to the work of Hanbury Brown and Twiss, discussed in Section 1.5, but was never explicitly utilized. However, Wolf[5] later discussed this theorem as a plausibility argument for their work.

To form the fourth-order correlation function, we can proceed by writing the two-point product of intensities in the far field using Equation (2.16) in a manner similar to that of Hanbury Brown and Twiss. However, to develop an approach adaptable to arbitrary orders of correlations, as well as to allow consideration of scattering surfaces with arbitrary roughness, we start by writing the fourth-order gaussian theorem (here for the electric-field spatial variable), where

$$\langle I(\underline{x}_1)I(\underline{x}_2)\rangle = \langle I(\underline{x}_1)\rangle \langle I(\underline{x}_2)\rangle + \left| \langle V(\underline{x}_1)V^*(\underline{x}_2)\rangle \right|^2, \qquad (2.33)$$

and where the angle brackets <> indicate a spatial average, not the more usual time average. We can conclude from Equation (2.33) that the second-order intensity correlation is composed of two terms, of which one forms the square of the second-order field correlation; the other is a spatial dc term, of no value here. Hanbury Brown and Twiss eliminated a similar temporal term by means of a dc block in their electronic apparatus. Part of the temporal dc signal contribution comes from terms in $\rho = 0$. The two-point product of intensities in the far-field (for $\rho = 0$) remains a constant in the time domain and is, therefore, of no utility in the Hanbury Brown - Twiss experiment. This two-point product does vary, however, as the spatial center-of-mass coordinate of the two points is translated over the detection plane. Thus, terms in $\rho = 0$ must be evaluated for the case of averaging in the spatial domain.

Using the moment reduction properties of Equation (2.33) along with Equation (2.32) and the more general form of the spatial-frequency correlation function expressed by Equation (2.25b), we can write

33

$$\langle I(\underline{x}_1,T)I(\underline{x}_2,T)\rangle = \left|\langle\Gamma(\underline{x}_1,\underline{x}_2;0;T)\rangle\right|^2, \tag{2.34a}$$

$$= \frac{1}{(cr)^4}\left|\int_0^\infty \sigma^2\,d\sigma \int_{-\infty}^\infty d\rho\ \text{sinc}(\rho T)H(\rho)\ \exp(i\rho r/c)\right.$$

$$\times \iiiint_{-\infty}^\infty \langle A(\underline{\xi}_1,\sigma)A(\underline{\xi}_2,\sigma)\ \exp[i\phi(\underline{\xi}_1-\underline{\xi}_2;\rho)]\rangle \tag{2.34b}$$

$$\times\ \exp\left[-i\left(\frac{\sigma+\rho/2}{rc}\right)\left(\underline{\xi}_1\cdot\underline{x}_1\right)\right]\exp\left[i\left(\frac{\sigma-\rho/2}{rc}\right)\left(\underline{\xi}_2\cdot\underline{x}_2\right)\right]d\underline{\xi}_1 d\underline{\xi}_2\Bigg|^2,$$

Next, we make the following transformation to spatial center-of-mass coordinates where

$$\underline{f} = \underline{\xi}_1 - \underline{\xi}_2 \quad\text{and}\quad \underline{g} = \frac{1}{2}(\underline{\xi}_1 + \underline{\xi}_2). \tag{2.35}$$

Introducing these into Equation (2.34), following some algebra, we find (suppressing constant terms),

$$\langle I(\underline{x}_1,T)I(\underline{x}_2,T)\rangle = \frac{1}{(cr)^4}\left|\int_0^\infty \sigma^2\,d\sigma \int_{-\infty}^\infty \text{sinc}(\rho T)H(\rho)\exp(i\rho r/c)d\rho\right.$$

$$\times \iiiint_{-\infty}^\infty \langle A(\underline{g}+\underline{f}/2,\sigma)A(\underline{g}-\underline{f}/2,\sigma)\exp[i\phi(\underline{f},\rho)]\rangle$$

$$\tag{2.36a}$$

$$\times\ \exp\left\{-i\left(\frac{\sigma+\rho/2}{rc}\right)\left[(\underline{g}+\underline{f}/2)\cdot\underline{x}_1\right]\right\}$$

$$\times\ \exp\left\{i\left(\frac{\sigma-\rho/2}{rc}\right)\left[(\underline{g}-\underline{f}/2)\cdot\underline{x}_2\right]\right\}d\underline{f}d\underline{g}\ \Bigg|^2$$

$$= \frac{1}{(cr)^4}\left|\int_0^\infty \omega^2\,d\omega \int_{-\infty}^\infty \text{sinc}(\rho T)H(\rho)d\rho\right.$$

$$\times \iint_{-\infty}^\infty I(\underline{\xi},\omega)\ \exp\left[-i\frac{k}{r}(\underline{x}_1-\underline{x}_2)\cdot\underline{\xi}\right]d\underline{\xi} \tag{2.36b}$$

$$\times \iint_{-\infty}^\infty C(\underline{f})\ \exp\left[-i\frac{k}{2r}(\underline{x}_1+\underline{x}_2)\cdot\underline{f}\right]d\underline{f}\ \Bigg|^2$$

34

$$\alpha \quad \left| \hat{I}\left[\frac{k}{r}(\underline{x}_1 - \underline{x}_2)\right]\right|^2 \left|\hat{C}\left[\frac{k}{2r}(\underline{x}_1 + \underline{x}_2)\right]\right|^2 \qquad (2.36c)$$

In going from Equation (2.36a) to Equation (2.36b), we have dropped the Fourier-transform terms in the difference frequency variable ρ, since they are clearly negligible in the far field. The ensemble average has been expressed as a product of two terms· $C(\underline{f})$ is a normalized phase correlation function[17] describing the coherence interval over a rough surface, and $I(\underline{\xi},\omega)$ is the intensity in the global-spatial variable. We have made the reasonable assumption that the field amplitude is constant within a given coherence area of the source; specifically, for $\underline{f}$ sufficiently small that $C(\underline{f}) \neq 0$, $A(\underline{g} + \underline{f}/2,\sigma) = A(\underline{g} - \underline{f}/2,\sigma) = A(\underline{g},\overline{\sigma}) = A(\underline{\xi},\sigma)$. This final approximation is made under the assumption that the coherence area of the source is small relative to the total source area, an assertion already made in an earlier argument for gaussian statistics. In Equation (2.36c), the circumflex indicates a two-dimensional spatial-Fourier transform.

In order to describe a spatially incoherent surface, $C(\underline{f})$ is usually allowed to assume the role of a delta function.[12] Thus, Equation (2.36) is reduced to a single integral in two space. Given this form, we see from Equation (2.36) that the spatial-averaged, two-point intensity correlation in the far field is proportional to the modulus of the spatial Fourier transform across a spatially rough surface, assuming a sufficiently short exposure time 2T. However, only for the case that the intensity distribution over the source has even symmetry can the phase of the spatial transform be inferred and used to invert uniquely Equation (2.36) to derive the intensity distribution on the source, $I(\underline{\xi},\omega)$.

Finally, the form of Equation (2.36c) shows explicitly that the intensity autocorrelation function in the far field is proportional to the product of two spatial power spectra. The spatial power spectrum $\left|\hat{I}\left[\frac{k}{r}(\underline{x}_1 - \underline{x}_2)\right]\right|^2$ is multiplied by $\left|\hat{C}\left[\frac{k}{2r}(\underline{x}_1 + \underline{x}_2)\right]\right|^2$, the spatial power spectrum of the correlation function describing the surface roughness. If the surface is sufficiently rough that this function approximates a delta function, then the transform is essentially constant, and all spatial frequencies of the source can be inferred. However, as the correlation interval increases, $\left|\hat{C}\left[\frac{k}{2r}(\underline{x}_1 + \underline{x}_2)\right]\right|^2$ acts to band limit the detectable spatial spectrum of the source. This effect is discussed, for example, by Kinsly[18] for the case of microdensitometer imaging with partially coherent light·

We also wish to point out that the transform of the intensity distribution over the source, $\hat{I}\left[\frac{k}{r}(\underline{x}_1 - \underline{x}_2)\right]$, is a function of the difference coordinates in the receiver space. However, the transform of the phase

35

correlation function, $\hat{C}\left[\frac{k}{2r}(\underline{x}_1 + \underline{x}_2)\right]$, is a function of the average (global) coordinates in the receiver space. This term cannot strictly come out of the spatial-averaging process of Equation (2.36), since the averaging is done in the global sense. In effect, the resolving capacity of a measurement in the receiver plane depends on the position in the plane. However, if the coherence area in the source plane is small, $\hat{C}$ is nearly constant over a large range of its argument and, hence, is generally insensitive to changes in the global space variable at the receiver around the origin. As indicated by Goodman,[17] this factor is generally treated as a constant over the receiving aperture.

2.7 An Illustrative Experiment

To illustrate the above ideas, we suggest a simple experiment embodying these mathematical ideas. A helium-neon laser in single-axial-mode configuration is used to transilluminate a symmetrical source (Figure 2.1). The source has a random-phase character to obtain spatial incoherence. The far-zone intensity pattern is recorded by film, using an exposure time less than the reciprocal of the source bandwidth. This exposure ensures that the spatial pattern is not washed out.
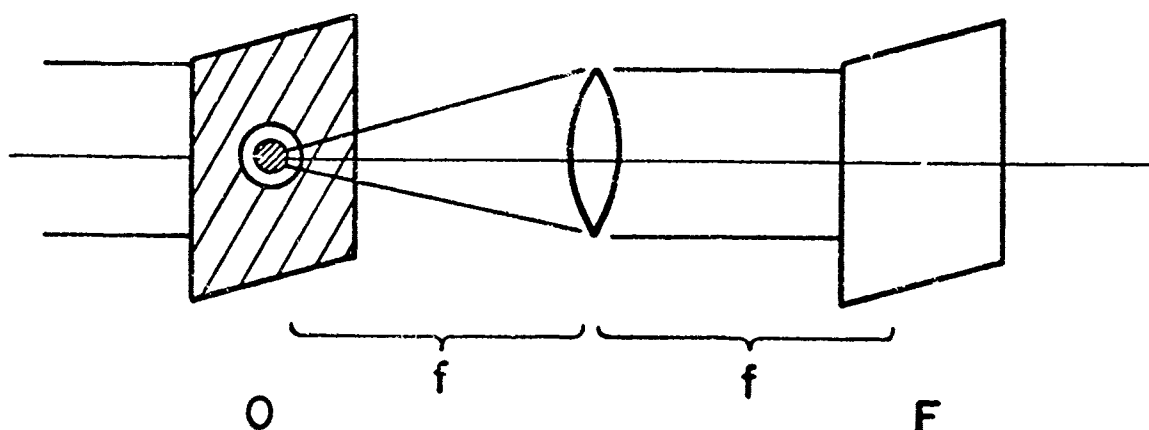

Figure 2.1 A symmetrical object (0) is illuminated with collimated light from a single-axial-mode laser. Ground glass is introduced at plane 0 to achieve spatial incoherence. The far-field intensity pattern is recorded by film at plane F. The lens focal length is indicated by f.

Next the film is developed so that it is linear in intensity and is used to make two identical positive transparencies. The positives are then placed in a collimated beam (Figure 2.2) to form the correlated intensity over an averaging area. The signal transmitted by the transparency pair is optically Fourier-transformed, a dc block is inserted
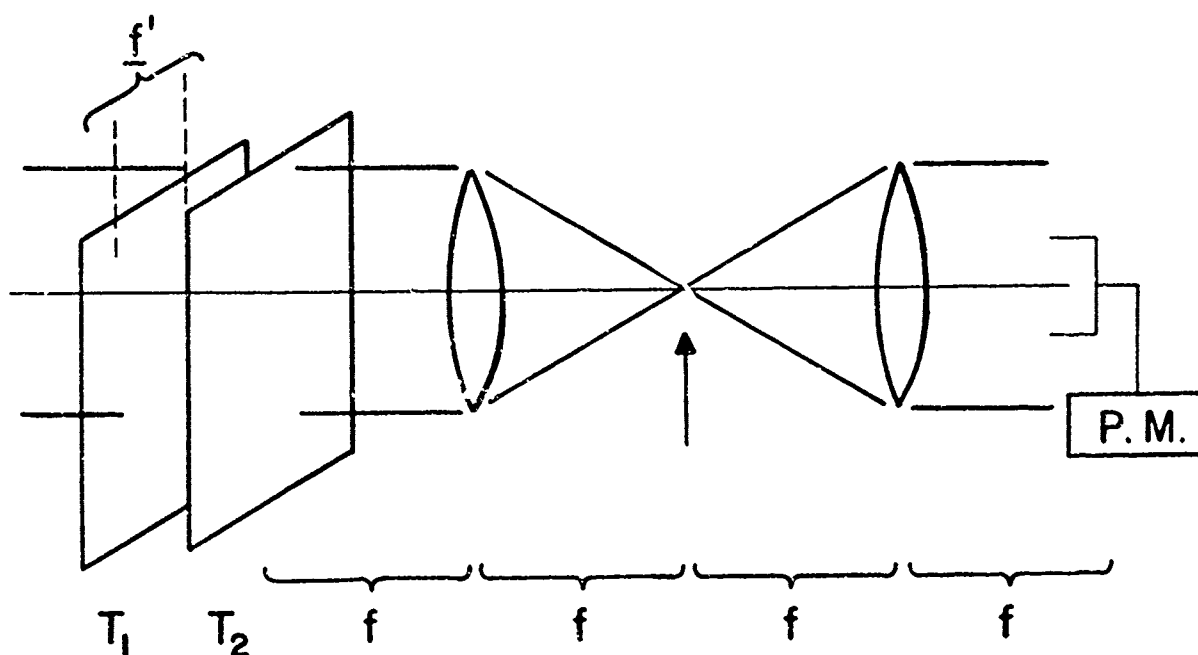
36

Figure 2.2 A pair of transparencies, T_1 and T_2, are made from film record in plane F of Figure 2.1. Intensity-autocorrelation function is measured by power meter for spatial lag $\underline{f}' = \underline{x}_1 - \underline{x}_2$. DC block is inserted between lenses at arrow to remove unwanted signal.

to remove the unwanted average term, and the total remaining irradiance is measured. This signal represents the mathematical expression given by Equation (2.36) for the transparency spatial lag, $\underline{f}' = \underline{x}_1 - \underline{x}_2$. Since the source is known, *a priori*, to be symmetrical, the transform of the source intensity is pure real. The square root of the correlation signal (see Section 3.4 for details of this operation) is proportional to the spectrum, which is then known as a function of spatial lag. Finally, this two-dimensional signal is Fourier-transformed by machine to give the scaled source irradiance.

2.8 Summary and Conclusions

Having developed an intermediate-average, mutual-coherence function as a starting point, we have derived an expression for the two-point intensity correlation in the far field, independent of time-averaging except for the temporal resolution of the detector. This result is valid for narrow-band, high-intensity light scattered from a spatially rough surface of arbitrary coherence area.

There are a number of special benefits from detecting images by the technique of intensity correlation. (1) The method is relatively insensitive to the effects of atmospheric scintillation.[2] (2) Because

37

the signal is detected in the spatial-transform domain, high-frequency
detail about the scattering surface translates to large spatial lags in
the far field. This result could be particularly important at frequencies where detector resolution is not well developed. (3) A special
advantage to intensity interferometry in the spatial domain is the utilization of gaussian statistics in the spatial (not temporal) sense. By
this method, sources with non-gaussian time statistics (such as single-axial-mode lasers) can be utilized. (4) Still another advantage of
spatial detection is that images of moving surfaces can be formed using
brief exposures.

We have therefore shown that, given a symmetrical, spatially incoherent source illuminated by high-intensity light, the far-zone intensity
pattern can be used to form the optical image of the source if the signal
is recorded with sufficiently short time resolution.

3. SPATIAL INTENSITY INTERFEROMETRY WITH SOURCES OF ARBITRARY SYMMETRY

3.1 Introduction

In Section 2, we showed that, given a symmetrical, spatially incoherent source illuminated by high-intensity light, the far-zone intensity
pattern can be used to form the optical image of the source if the signal
is recorded with sufficiently short time resolution. The primary result
of this analysis is that the far-field intensity correlation function is
proportional to the square of the spatial Fourier transform of the source
intensity distribution. Since, in general, a source exhibits an intensity profile of arbitrary symmetry, its spatial Fourier transform is complex. The measurement, however, gives information only about the spatial
power spectrum (absolute square of the spatial Fourier transform) and,
therefore, only the modulus of the Fourier transform can be inferred.
The inversion of the spatial transform to derive the source intensity is
thus impossible since the necessary phase information has been lost.

In the experiments of Hanbury Brown and Twiss, the loss of phase is
not a serious limitation since their objective is simply the measurement
of star diameters. If a circular disk is used as a model for a star, the
object is known, *a priori*, to be symmetrical. Thus the spatial transform
of the (real) intensity is pure real. For this situation, the phase of
the transform is zero or π for all spatial wave numbers, and the square
root of the power spectrum can be taken (with a sign ambiguity to be discussed below) to derive the spatial transform itself.

In the application of intensity-interferometric techniques to terrestrial imaging systems, though, the loss of phase is a serious limitation to the method. A number of authors[19,20,21] have addressed
themselves to the problem of phase recovery. Wolf[19] pointed out that
the complex transform of intensity has analytical properties that can
be used in certain situations to infer the phase from measurements of

38

the modulus alone. Gamo[10,22] has suggested a triple-intensity correlation scheme by which the phase can be inferred. However, there is an ambiguity in the sign of the phase angle, and two intensity profiles are derived, one the symmetrical inverse of the other, and supplementary information must be gathered to infer the proper-handed image. Mehta[23] has proposed another scheme in which a reference beam of an exactly known complex degree of coherence is superimposed on the signal beam.

We suggest here a simple technique which, when used with spatial detection, gives both the amplitude and phase of the transform. This method utilizes preprocessing of the electric field before detection to exploit a symmetry property of Fourier transform theory.

3.2 A Symmetry Property

We start by reviewing the well-known property that a function $f(x)$ can be represented by a sum of two functions,[24] one of which is the even (symmetrical) part of $f(x)$, and the other the odd. The even $[E(x)]$ and odd $[O(x)]$ parts of $f(x)$ can be found simply by the formulas

$$E(x) = \frac{1}{2} [f(x) + f(-x)] \qquad (3.1a)$$

and

$$O(x) = \frac{1}{2} [f(x) - f(-x)]. \qquad (3.1b)$$

If, in addition, we know that $f(x)$ is pure real, then the Fourier transform will be hermitian; that is, the transform of the even part of $f(x)$, $\hat{E}$, will be pure real, while the transform of the odd part will be pure imaginary.[24]

By the spatial-intensity method noted, the modulus of the Fourier transform of the source intensity can be derived. Using the above symmetry properties, we preprocess the electric field before detection and autocorrelation so that the source is effectively symmetrized in its intensity profile. Since its transform is pure real, the power spectrum can be used to compute the spectrum of the even part of the source irradiance. The Fourier spectrum of the even part of the source intensity is, however, the real part of the transform of the unpreprocessed signal. Thus, if the modulus and the real part of the transform for each spatial wave number are compared, the phase of the transform can be inferred to within a sign and used to compute the source intensity. The removal of the sign ambiguity will be discussed below.

3.3 Mathematical Model

We start by writing a symmetrized field in the far zone of the source $(\underline{\xi})$ plane, where

$$V_E(\underline{x}_i) \equiv V(\underline{x}_i) + V(-\underline{x}_i). \qquad (3.2)$$

39

Writing the correlation of $I'(\underline{x}_1)$ and $I'(\underline{x}_2)$, where $I'(\underline{x}_i) \equiv V_E(\underline{x}_i)V_E^*(\underline{x}_i)$, and using the theorem of gaussian statistics [Equation (1.13)], we have

$$\langle I'(\underline{x}_1)I'(\underline{x}_2)\rangle = |\langle V_E(\underline{x}_1)V_E^*(\underline{x}_2)\rangle|^2 \tag{3.3a}$$

$$= |\langle V(\underline{x}_1)V^*(\underline{x}_2) + V(\underline{x}_1)V^*(-\underline{x}_2) + V(-\underline{x}_1)V^*(\underline{x}_2) + V(-\underline{x}_1)V^*(-\underline{x}_2)\rangle|^2,$$

$$\tag{3.3b}$$

where constant terms here and in later expressions have been suppressed. Now the form of Equation (2.34b) is used to express the intensity correlation to get

$$\langle I'(\underline{x}_1;T)I'(\underline{x}_2;T)\rangle = \left| \int_0^\infty \sigma^2 d\sigma \int_{-\infty}^\infty \text{sinc}(\rho T)H(\rho)\ \exp(i\rho r/c)d\rho \right.$$

$$\times \iiiint_{-\infty}^\infty \left\{ \langle A(\underline{\xi}_1,\sigma)A(\underline{\xi}_2,\sigma)\ \exp[i\phi(\underline{\xi}_1 - \underline{\xi}_2;\rho)]\rangle \right.$$

$$+ \langle A(\underline{\xi}_1,\sigma)A(-\underline{\xi}_2,\sigma)\ \exp[i\phi(\underline{\xi}_1 + \underline{\xi}_2;\rho)]\rangle$$

$$+ \langle A(-\underline{\xi}_1,\sigma)A(\underline{\xi}_2,\sigma)\ \exp[i\phi(-\underline{\xi}_1 - \underline{\xi}_2;\rho)]\rangle \tag{3.4}$$

$$\left. + \langle A(-\underline{\xi}_1,\sigma)A(-\underline{\xi}_2,\sigma)\ \exp[i\phi(-\underline{\xi}_1 + \underline{\xi}_2;\rho)]\rangle \right\}$$

$$\left. \times \exp\left[-i\left(\frac{\sigma + \rho/2}{rc}\right)\left(\underline{\xi}_1 \cdot \underline{x}_1\right)\right] \exp\left[i\left(\frac{\sigma - \rho/2}{rc}\right)\left(\underline{\xi}_2 \cdot \underline{x}_2\right)\right]d\underline{\xi}_1 d\underline{\xi}_2 \right|^2.$$

We can see now that the form of the intensity correlation in the far field is proportional to the square of the spatial Fourier transform of four terms. The nature of these terms can be better understood by referring to Figure 3.1a. We show the coordinate axes for the source ($\underline{\xi}$) plane. Two points $\underline{\xi}_1$ and $\underline{\xi}_2$ and their symmetrical pair are represented. The circle illustrates the coherence area characterizing the surface roughness. As discussed in Section 2, the first average of Equation (3.4) is zero unless points $\underline{\xi}_1 = \underline{\xi}_2$ such that they can be enclosed by the perimeter of the coherence area. If this criterion is satisfied for the first average, it is also met for the last. Similarly, the cross products of Equation (3.4) are zero unless $\pm\underline{\xi}_1 = \mp\underline{\xi}_2$.
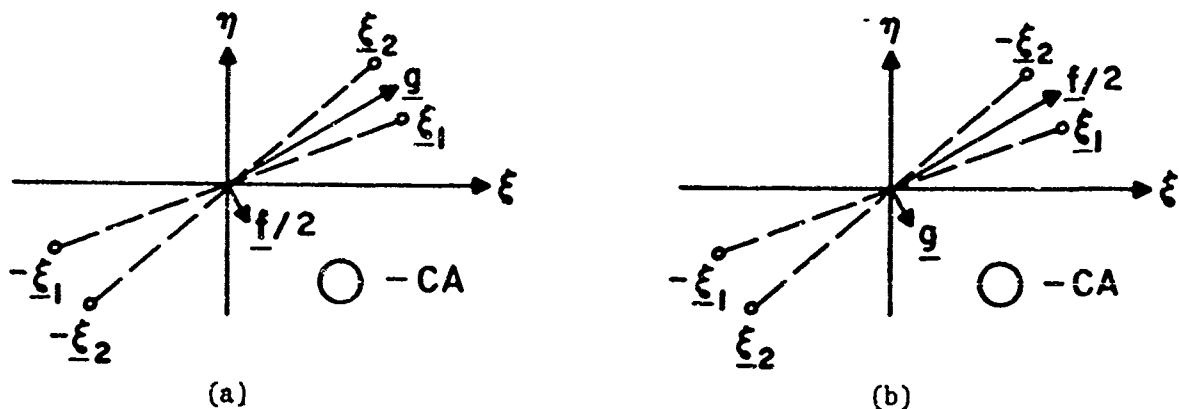
40

Figure 3.1 Coordinate axes in the plane of the source. (a) Points ξ_1 and ξ_2 and their symmetrical pair are shown; center-of-mass vectors are shown, where $\underline{g}$ is the mean of positions ξ_1 and ξ_2 and $\underline{f}$ is the difference. For the coherence area (CA) small, $\underline{g} = \xi_1 = \xi_2 = \xi$, and $\underline{f} = 0$. (b) Source-plane coordinates for $\xi_1 = -\xi_2$. Here the center-of-mass vectors indicate $\underline{g} = 0$ and $\underline{f}/2 = \xi_1 = -\xi_2$.

We also wish to note that the spatial average expressed by the angle brackets on the left-hand side of Equation (3.4) can be assumed to approach the ensemble average as the area of spatial correlation in the detector plane grows large with respect to the correlation interval in the same plane. The nature of this correlation function is such that information about the individual intensity products $[I'(\underline{x_i};T)I'(\underline{x_j};T)]$ will be averaged over the active correlation area. To understand this average more fully, we define center-of-mass coordinates in the receiver plane where

$$\underline{g}' \equiv \frac{\underline{x}_1 + \underline{x}_2}{2} \quad \text{and} \quad \underline{f}' \equiv \underline{x}_1 - \underline{x}_2. \qquad (3.5)$$

Thus the intensity correlation in the far zone can be expressed functionally as

$$\langle I'(\underline{x}_1;T)I'(\underline{x}_2;T)\rangle = \langle I'(\underline{g}' + \underline{f}'/2;T)I'(\underline{g}' - \underline{f}'/2;T)\rangle. \qquad (3.6)$$

But for a particular spatial correlation lag, the difference between receiver points, $\underline{f}'$, will remain constant while the center of mass of the points, $\underline{g}'$, will vary. Depending on the domain over which $\underline{g}'$ is varied, terms dependent on this global variable should disappear leaving only functions of the difference coordinate.

We now examine the first and last terms $(T_{1,4})$ of Equation (3.4). If we change the position variables over the source, ξ_1 and ξ_2, to

center-of-mass coordinates, $\underline{g}$ and $\underline{f}$, in the manner of Equation (3.5), we get for these terms

$$T_{1,4} = \iiiint\limits_{-\infty}^{\infty} \left\{ \langle A(\underline{g} + \underline{f}/2, \sigma) \; A(\underline{g} - \underline{f}/2, \sigma) \; \exp[i\phi(\underline{f})] \rangle \right.$$

$$\left. + \; \langle A(-\underline{g} - \underline{f}/2, \sigma) \; A(-\underline{g} + \underline{f}/2, \sigma) \; \exp[i\phi(-\underline{f})] \rangle \right\} \qquad (3.7)$$

$$\times \; \exp[-i \frac{\sigma}{rc} \; (\underline{g} + \underline{f}/2) \cdot \underline{x}_1] \; \exp[i \frac{\sigma}{rc} \; (\underline{g} - \underline{f}/2) \cdot \underline{x}_2] d\underline{g} d\underline{f}.$$

As discussed in Section 2, the form of Equation (3.7) implies that the amplitude and phase of the fields at the source can be expressed in product form. The character of the spatial incoherence is determined by the exponential terms within the angle brackets that form the phase correlation function over the source. Since we assume a small coherence area relative to the source dimensions, here in Equation (3.7), $\underline{f}$ is small such that $A(\underline{g} + \underline{f}/2, \sigma) \approx A(\underline{g} - \underline{f}/2, \sigma) \approx A(\underline{g}, \sigma)$. Figure 3.1a illustrates the center-of-mass vectors. For terms $T_{1,4}$ to have value, $\underline{f}$ must be small so that $|\underline{\xi}_1 - \underline{\xi}_2|$ is less than the diameter of the source coherence area. We have also dropped the Fourier transform terms in the temporal difference frequency variable, ρ. With these approximations, the first bracketed expression can be written

$$\langle A(\underline{g} + \underline{f}/2, \sigma) \; A(\underline{g} - \underline{f}/2, \sigma) \; \exp[i\phi(\underline{f})] \rangle$$

$$= \langle [A(\underline{g}, \sigma)]^2 \rangle \; \langle \exp[i\phi(\underline{f})] \rangle \qquad (3.8a)$$

$$= \; I(\underline{g}, \omega) \; C(\underline{f}), \qquad (3.8b)$$

where the center-of-mass temporal frequency, σ, has been changed in Equation (3.8b) to ω. With a similar development of the second bracketed expression, Equation (3.7) can be written

$$T_{1,4} = \iint\limits_{-\infty}^{\infty} [I(\underline{g}) + I(-\underline{g})] \; \exp\left\{-i \frac{k}{r} [\underline{g} \cdot (\underline{x}_1 - \underline{x}_2)]\right\} d\underline{g}$$

$$\times \iint\limits_{-\infty}^{\infty} C(\underline{f}) \; \exp\left\{-i \frac{k}{r} \; \underline{f}/2 \cdot (\underline{x}_1 + \underline{x}_2)\right\} d\underline{f}, \qquad (3.9a)$$

$$= \; \hat{I}_E \left[\frac{k}{r} \; (\underline{x}_1 - \underline{x}_2) \right] \; \hat{C} \left[\frac{k}{2r} \; (\underline{x}_1 + \underline{x}_2) \right]. \qquad (3.9b)$$

42

Here k is the wave number of the light, and we have used the evenness of $C(\underline{f})$ to separate the two integrals. The circumflexes in Equation (3.9b) indicate a spatial Fourier transform, and $I_E = I(\underline{\xi}) + I(-\underline{\xi})$, a symmetrized source intensity distribution (since $\underline{\xi}_1 \approx \underline{\xi}_2 \approx \underline{g} \approx \underline{\xi}$).

In a similar manner, the second and third terms in Equation (3.4) can be examined to get

$$T_{2,3} = \hat{I}_E\left[\frac{k}{r}\,(\underline{x}_1 + \underline{x}_2)\right]\,\hat{C}\left[\frac{k}{2r}\,(\underline{x}_1 - \underline{x}_2)\right]. \tag{3.10}$$

Figure 3.1b indicates the position of the center-of-mass vectors for this term. Here $\underline{\xi}_1 \approx \underline{\xi}_2$ so that $\underline{g}$ is small and $\underline{f}/2 \approx \underline{\xi}_2 \approx \underline{\xi}_1$. The results of Equations (3.9) and (3.10) show that the symmetrization and multiplication processes lead to two spatial Fourier transforms of a symmetrized source intensity. One term depends on the difference of coordinates in the far-zone (is spatially invariant); the other depends on the global term. Since the spatial average of Equations (3.4) and (3.6) involves the translation of the global variable in the receiver coordinates, term $T_{2,3}$ of Equation (3.10) is summed to a constant and contributes only for small global sizes and can be neglected in comparison to $T_{1,4}$ for large global excursions. This result is true only for the spatial-average case. This can be seen by noting that the transverse receiver correlation lag for optical sources in the far field is typically a few millimetres. Under the assumption of a large averaging area, this means that term $T_{2,3}$ would contribute only for $g' < 3$ mm, while term $T_{1,4}$ would contribute for all g' up to the limit imposed by $\hat{C}\left[\frac{k}{2r}\,(\underline{x}_1 + \underline{x}_2)\right]$. The transform of the symmetrized source intensity expressed in Equation (3.9b) is space invariant. However, $\hat{C}$, the transform of the phase correlation, is a function of the global variable. As discussed earlier, the correlation function $C(\underline{f})$ approaches a delta function if the criterion of spatial incoherence is applied to the surface roughness over the source. Thus its transform, $\hat{C}(g')$, is nearly constant over a wide band of spatial frequencies. Therefore, $\hat{C}(g')$ is relatively insensitive to changes in its argument over wide ranges of spatial wave number. But the argument of $\hat{C}$ is, in general, different for each pair of multiplied intensities in the far field. Depending on the bandwidth of $\hat{C}$, the maximum averaging area can be specified so that no band limiting occurs for the maximum global variation.

Apparently the term of Equation (3.10) arises because of the way in which the source was symmetrized. When a source is considered symmetrical, it is the intensity only which is symmetrical about the origin. However, here, by the nature of the field symmetrization at the receiver, there are two positions for which the phase correlation function is unity rather than the usual one. The cross terms that form $T_{2,3}$ give a scaling to the Fourier transform that is quite different from the term $T_{1,4}$.

43

Using the results of Equation (3.9b) and the fact that the term of Equation (3.10) sums to a negligible constant under a spatial average, we can finally write the correlation of intensities $I'(\underline{x}_1;T)$ and $I'(\underline{x}_2;T)$

$$
\langle I'(\underline{x}_1;T)I'(\underline{x}_2;T)\rangle = \left| \int_0^\infty \omega^2 d\omega \int_{-\infty}^\infty \text{sinc}(\rho T)H(\rho)d\rho \right.
$$

$$
\times \iint_{-\infty}^\infty I_E(\underline{\xi},\omega) \exp[-i\frac{k}{r}(\underline{x}_1-\underline{x}_2)\cdot\underline{\xi}]d\underline{\xi} \qquad (3.11a)
$$

$$
\times \left. \iint_{-\infty}^\infty C(\underline{f}) \exp[-i\frac{k}{2r}(\underline{x}_1+\underline{x}_2)\cdot\underline{f}]\, d\underline{f} \right|^2
$$

$$
\propto \left| \hat{I}_E\left[\frac{k}{r}(\underline{x}_1-\underline{x}_2)\right] \right|^2 \left| \hat{C}\left[\frac{k}{2r}(\underline{x}_1+\underline{x}_2)\right] \right|^2, \qquad (3.11b)
$$

where Equation (3.11b) is written with the understanding that $\left|\hat{C}\left[\frac{k}{2r}(\underline{x}_1+\underline{x}_2)\right]\right|^2$ weights $\left|\hat{I}_E\right|^2$ in a non-stationary way over the receiver plane and is, hence, not strictly separable. However, this term is generally treated as a constant over the receiver plane.[17] In this equation, $I_E(\underline{\xi},\omega) = I(\underline{\xi},\omega) + I(-\underline{\xi},\omega)$ which, by Equation (3.1a), is the even part of the source intensity. In Equation (3.11b), $\left|\hat{I}_E\left[\frac{k}{r}(\underline{x}_1-\underline{x}_2)\right]\right|^2$ is the spatial power spectrum of the even part of the source intensity distribution and $\left|\hat{C}\left[\frac{k}{2r}(\underline{x}_1+\underline{x}_2)\right]\right|^2$ is the spatial power spectrum of the source phase correlation function.

This information will be used below to form the image $I(\underline{\xi},\omega)$.

3.4 The Transform Inversion

Using the results of Equation (3.11) and the modulus of the total transform, we can now find the intensity distribution on the source, $I(\underline{\xi},\omega)$. In Figure 3.2a, we illustrate the measured spatial power spectrum derived by the method of Section 2. If the (positive) square root is taken, the modulus of the transform (Figure 3.2b) is known. Figure 3.3a illustrates the spatial power spectrum of the even part of the source intensity derived in Equation (3.11). By the hermitian property of the transform,[24] the spectrum itself is pure real. We take the square root (Figure 3.3b), but with a sign ambiguity such that two spectra are derived, one the negative of the other. The proper spectrum can be inferred, however, on the basis of the central-ordinate property of the Fourier transform (Ref. 24, p. 136), whereby the definite integral of a function over infinite limits in one space is equal to the value of of its transform at the origin. Since the intensity is a positive-definite function, the proper spectrum is positive at the origin.
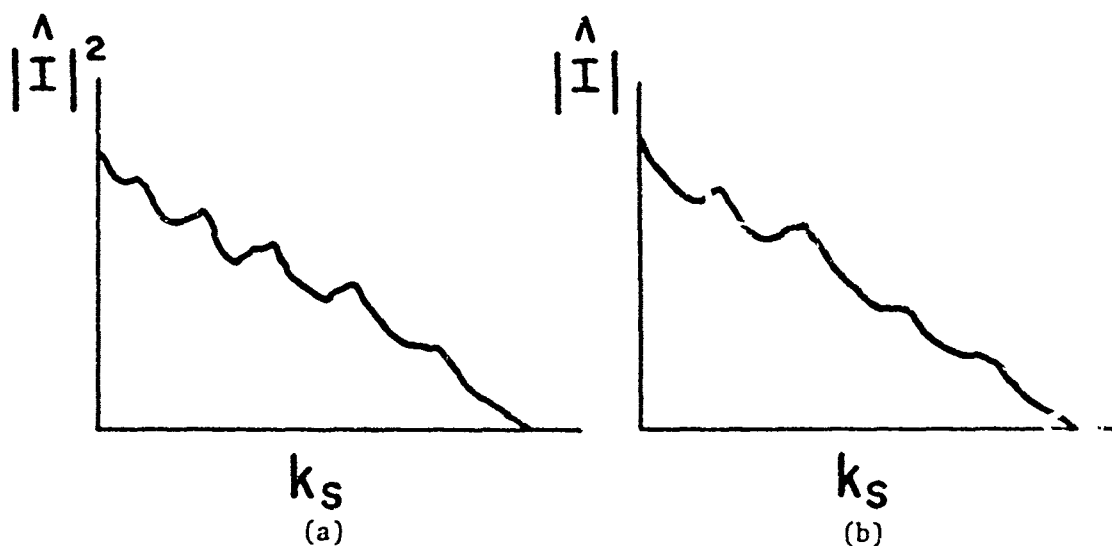
44

Figure 3.2 (a) Representation of spatial power spectrum of source intensity distribution, $|\hat{I}|^2$, vs. spatial wave number k_S. (b) Modulus of power spectrum, $|\hat{I}|$, vs. spatial wave number k_S.
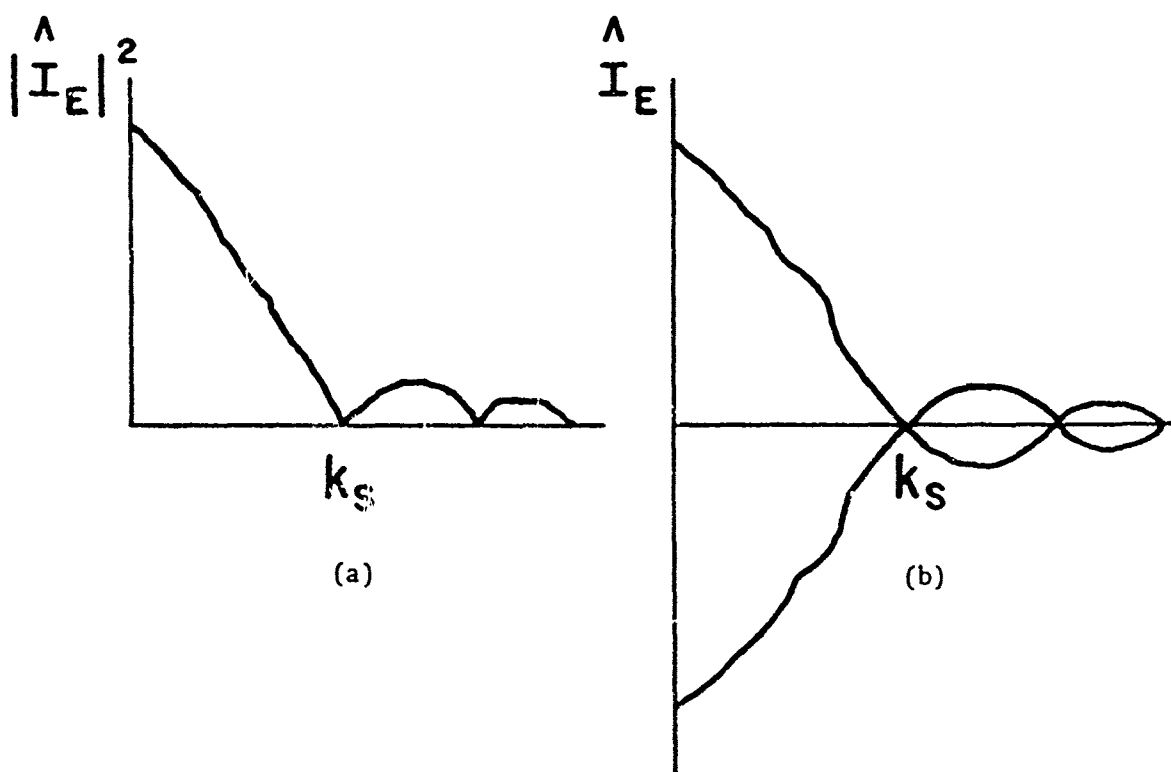

Figure 3.3 (a) Power spectrum of even part of source distribution. (b) Two possible real spectra of the even part of the source distribution. The spectrum which is negative for $k_S = 0$ can be eliminated.

Now, using Figures 3.2b and 3.3b, we know the modulus and the projection on the real axis for each spatial wave number k_{oS}. Figure 3.4
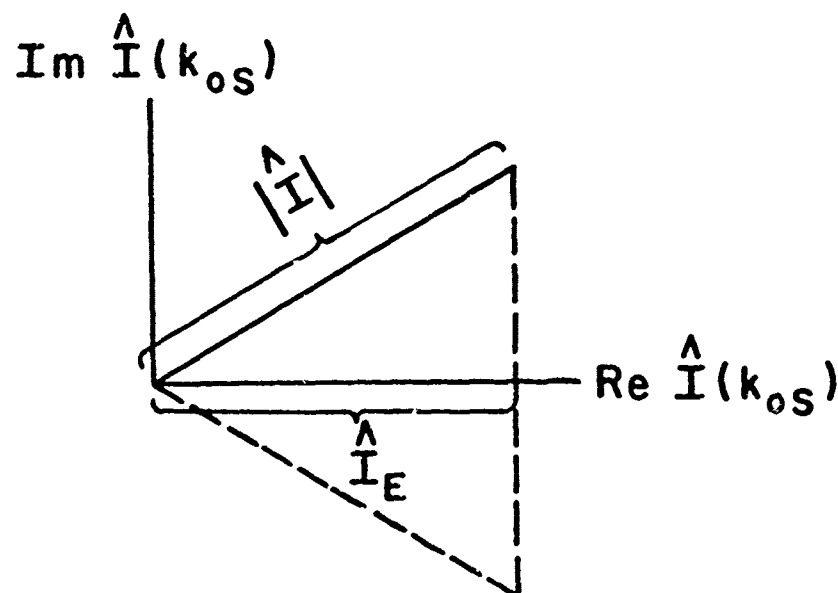
Figure 3.4 For a particular spatial wave number, k_{oS}, the modulus and its projection on the real axis, $\hat{I}_E$, are shown. As indicated by the lower dotted line, the modulus could be located in the lower-half plane, thus giving two possible values for the phase of the transform.

illustrates this point by showing the length of the modulus, $|\hat{I}|$, and its projection (possibly negative), $\hat{I}_E$, on the real axis. It should be noted that there is also a sign ambiguity here in the phase angle, for the modulus could appear in the upper- or lower-half plane. From the present information, there appears to be no way to resolve the sign of the phase angle. Thus two phases are derived, one the negative of the other. If each phase record is used with the modulus in a Fourier inversion operation, two images are derived, one the symmetrical inverse (reflection through the origin) of the other, much the same as Gamo found by a triple-correlation technique.[10,22]

However, in practice, the choice of the proper (erect) image would seem to be straightforward through the use of a further property of the Fourier transform. The first moment of a function can be shown to be (Ref. 24, p. 138)

$$\int_{-\infty}^{\infty} x f(x) dx = \frac{F'(0)}{-2\pi i} , \qquad (3.12)$$

where $F'(0)$ is the first derivative of the transform of $f(x)$ evaluated at the origin. It should be noted that, here, origin refers to the point

46

where the argument of the F' function is zero; it does not imply that the derivative is inferred through a measurement constrained to the neighborhood of the origin in the receiver coordinates. Substituting $I(\xi)$ for $f(x)$, the operation of Equation (3.12) describes the point where $I(\xi)$ is mainly concentrated. Since, in practice, we can always translate the source in a known direction off axis by pointing the receiver system, the source can be moved into, say, the right-half plane. This means that the centroid is positive, such that the slope of the spectrum must be negative at the origin. Using this information in Figure 3.4 for the spatial wave number $k_{oS} = 0$, we can choose the phase plot with negative slope. Thus the proper orientation of the image is inferred, and the source intensity distribution is completely specified.

We note that in these operations the Whittaker-Shannon sampling theorem must be considered with respect to both the spatial-frequency content of the source and its position relative to the axis of the viewing system. The method here depends on the unique inference of two spectra by means of the preprocessed detection scheme. The behavior of the spectra as inferred from the power spectra is particularly critical as the functions approach zero crossings. There the ambiguity of the functions must be inferred on the basis of continuity arguments. Thus the limitation on the method appears to depend on noise in the process which might obscure the behavior at these critical points. Also, by the effect of the shift theorem,[24] even a low spatial-frequency source when positioned off axis would exhibit fast phase variation, causing the spectra to go through many zero crossings.

There is a second method of data reduction that is more expedient than the above dual operation. If the object is pointed sufficiently far off axis such that the twin images of the symmetrized field do not overlap, then the standard processing leading to the modulus of the transform can be ignored. The intensity record from the symmetrized field can be used to form the twin images, since the transform is pure real, using the criteria of Figure 3.3 to resolve the proper sign of the square root. After reconstruction, one of the images can be discarded.

3.5 Measurement Technique

The operation of Equation (3.2) must be accomplished in real time before intensity detection. Wessely and Bolstad,[25] in a study of turbulence-induced phase fluctuations, have utilized an optical device that achieves such field symmetrization. A beam-splitter cube, illustrated in Figure 3.5, divides the incoming wave (I) into two parts, each of which is inverted by right-angle prisms rotated 90° with respect to each other. After recombination, the field (at F) has the form of Equation (3.2). We note that the ray paths for each leg of the splitter-inverter undergo an odd number of reflections; hence, with respect to the incident wave, the recombined field at F exhibits a change in handedness in both the inverted and non-inverted images. The proper handedness can be restored, of course, by utilizing an additional planar reflection. In an actual application, it is likely that the splitter-recombiner would
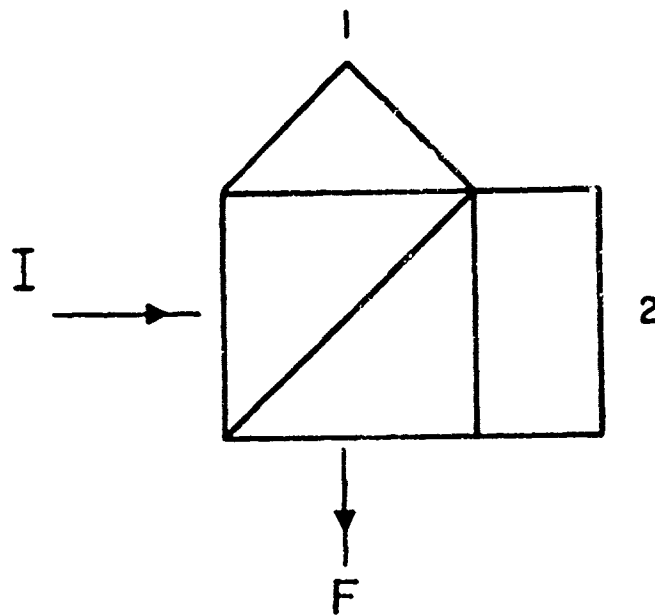
47

Figure 3.5 Beam-splitter cube that divides the
wave into two parts, each of which is inverted
by right-angle prisms (1,2) rotated 90° with
respect to each other. After recombination at
F, the electric field has the form of Eq. (3.2).

be preceded by a telescope, a practical necessity to reduce unwanted
background illumination and to increase the effective size of the detec-
tion plane. In contrast to the experiment of Hanbury Brown and Twiss,
the optical parts preceding the detector plane would have to be high
quality.

The inversion operation described in Section 3.4 can, of course, be
accomplished by electronic processing following reading of the intensity
records. It is not clear how purely optical techniques could be used,
since there is a series of decisions that must be made involving signs
of square roots and continuity of functions at zero (abscissa) crossings.

3.6 Summary and Conclusions

We have shown that by preprocessing the electric field in a simple
way to gain symmetry, the technique of intensity interferometry can be
used to derive the intensity profile of a source of arbitrary symmetry.
This result is accomplished by comparing the intensity-correlation func-
tions of the processed and normal intensity records. It is interesting
to note that it is not necessary to invoke the methods of higher-order
correlations[10,22] to infer the phase of the spatial transform.

48

4. LASER SPECKLE AND SPATIAL INTENSITY INTERFEROMETRY

4.1 Introduction

In this section, we will discuss the relationship between the well-known phenomenon of laser speckle and spatial intensity interferometry. There is a strong similarity between the results derived in Section 2 and previous analyses dealing with laser speckle; both areas of theory show that the absolute square of the source-intensity Fourier transform is proportional to the far-field correlation of intensities. Although the mathematical relations between the source and detection planes are similar, the intensity signals at the detection plane that are auto-correlated arise from different phenomena. Laser speckle theory is formulated in terms of a monochromatic field scattered from a rough sur-face. The time-invariant speckle pattern in the far field originates from the interference of monochromatic waves from different points over the scattering surface. Spatial intensity interferometry is formulated in terms of quasimonochromatic radiation scattered from a rough surface. A time-dependent speckle pattern in the far field is generated by inter-ference of different temporal frequencies scattered from the source. Thus the temporal response of the detector must be sufficiently short to resolve the time-varying, intensity-interferometric signal. However, the time-invariant speckle pattern can be recorded with a long exposure.

We will discuss the mathematical similarities between these two theories.

4.2 Laser Speckle Formulation

Two papers, representative of laser-speckle investigations, are due to Goldfischer[26] and Crane.[27] Although there are some discrepancies in the results of these efforts,[27] the basic conclusions are similar. To illustrate the results of laser speckle, we use the work of Goldfischer.

We start by noting that Goldfischer argues for a diffuse surface model that contains 'an infinitely dense collection of scatterers...with random phases." He has thus implicitly argued for the criterion of spa-tial incoherence even though he does not utilize this concept in a quan-titative way [cf. Equation (1.7b)]. Goldfischer begins with a real form of the Huygens-Fresnel equation (cf. Section 1.2) by writing the electric field in the receiver plane as

$$E(x,y) = \left[\frac{\alpha I(\xi,\eta)\Delta\xi\Delta\eta}{\pi r^2}\right]^{\frac{1}{2}} \cos\left[k\left(ct + \frac{x\xi + y\eta}{r}\right) + \theta_{xy} + \psi_{\xi\eta}\right], \qquad (4.1)$$

where the field, $E(x,y)$, is due to the particular area on the scatterer at $\Delta\xi\Delta\eta$, $\psi_{\xi\eta}$ is a random phase angle associated with the scatterer at (ξ,η), and θ_{xy} is a coefficient written to absorb the terms neglected in

Equation (1.2b) and depends on the location of the point of observation, and α is the scattering efficiency of the surface. We note that Equation (4.1) reveals a monochromatic treatment of the scattered laser radiation.

Next, the field at the receiver plane is squared to form the intensity, giving

$$I(x,y) = \frac{\alpha \Delta\xi \Delta\eta}{2\pi r^2} \sum_{\xi,\eta} \sum_{\xi',\eta'} [I(\xi,\eta)I(\xi',\eta')]^{\frac{1}{2}}$$

$$\times \left\{ \cos\left[k\left(\frac{x\xi + y\eta}{r}\right) + \psi_{\xi\eta}\right] \cos\left[k\left(\frac{x\xi' + y\eta'}{r}\right) + \psi_{\xi'\eta'}\right] \right. \quad (4.2a)$$

$$\left. + \sin\left[k\left(\frac{x\xi + y\eta}{r}\right) + \psi_{\xi\eta}\right] \sin\left[k\left(\frac{x\xi' + y\eta'}{r}\right) + \psi_{\xi'\eta'}\right] \right\}$$

$$= \frac{\alpha \Delta\xi \Delta\eta}{2\pi r^2} \sum_{\xi,\eta} \sum_{\xi',\eta'} [I(\xi,\eta)I(\xi',\eta')]^{\frac{1}{2}} \quad (4.2b)$$

$$\times \cos\left[k\,\frac{x(\xi - \xi') + y(\eta - \eta')}{r} + (\psi_{\xi\eta} - \psi_{\xi'\eta'})\right].$$

The summations of Equation (4.2) are later allowed to approach integrals as the areas $\Delta\xi\Delta\eta$ go to zero. There are two distinct forms for this equation. If the primed terms are equal to the unprimed terms, the mean intensity in the far field is derived. This is the dc term of no use to us here. The intensity $I(x,y)$ of utility here has the mean subtracted out, and we restrict, as does Goldfischer, the summations of Equation (4.2) to occur only over the unequal primed and unprimed variables, i.e., we require $\xi \neq \xi'$ and/or $\eta \neq \eta'$.

We now define new variables of integration

$$\frac{k}{r}(\xi - \xi') = \omega \quad \text{and} \quad \frac{k}{r}(\eta - \eta') = \Omega. \quad (4.3)$$

Using these relations, the spatial intensity autocorrelation function in the far field of the source is formed, where averaging eliminates terms involving random phases to give

50

$$\langle I(\underline{x}_1) I(\underline{x}_2) \rangle = \frac{1}{8} \left[\frac{\alpha}{\pi k r} \right]^2 \int\int\limits_{-\infty}^{\infty} d\omega \, d\Omega \, \cos(\omega\gamma + \Omega\delta)$$

$$\times \int\int\limits_{-\infty}^{\infty} d\xi \, d\eta \, I(\xi,\eta) \, I(\xi - \frac{r}{k} \omega, \, \eta - \frac{r}{k} \Omega), \qquad (4.4)$$

and the spatial lag in the detector plane is expressed by

$$\gamma = x_1 - x_2 \quad \text{and} \quad \delta = y_1 - y_2. \qquad (4.5)$$

Thus the right-hand side of Equation (4.4) expresses the autocorrelation of intensities in the far field as a Fourier transform of the auto-correlation of intensities over the source.

Finally, using the autocorrelation theorem, Equation (4.4) can be written in the form given by Goldfischer where

$$\langle I(\underline{x}_1) \, I(\underline{x}_2) \rangle = (\alpha^2/8\pi r^4) \, |\hat{I}(\gamma,\delta)|^2, \qquad (4.6)$$

and

$$\hat{I}(\gamma,\delta) = \int\int\limits_{-\infty}^{\infty} d\xi \, d\eta \, I(\xi,\eta) \, \exp\left[i \, \frac{k}{r} \, (\gamma\xi + \delta\eta) \right]. \qquad (4.7)$$

This result, utilizing only a monochromatic formulation, is identical in form to the comparative expression of spatial intensity interferometry given in Equation (2.36); the intensity autocorrelation function in the far zone of a spatially incoherent source is proportional to the absolute square of the spatial Fourier transform over the source. However, Equation (4.6) reflects no constraint involving the exposure time. As indicated by Equation (4.2b), the useful intensity signals in the receiver plane arise from interference of monochromatic waves over different portions of the source plane.

4.3 Summary and Conclusions

We have seen that both laser speckle and spatial intensity inter-ferometry techniques indicate that the far-field correlation of intensi-ties is proportional to the absolute square of the source-intensity Fourier transform. However, laser speckle theory describes scattered monochromatic radiation in a time-independent pattern requiring no expo-sure control to detect. In contrast, spatial intensity interferometry is formulated in terms of quasimonochromatic radiation that yields a time-varying pattern. Exposure control commensurate with the bandwidth of the radiation is required to resolve the pattern.

51

We have seen that both the time-varying and time-invariant speckle patterns contribute to the useful signal describing the source intensity distribution. We must ask, is it to be expected that speckle recording with short exposures would result in an increased signal in the auto-correlation process due to the time-varying signal which would otherwise be lost? It would seem that the answer lies in the nature of the correlation between the two kinds of patterns. This question will be examined experimentally in the next section.

5. EXPERIMENTS IN INTENSITY CORRELATIONS

5.1 Introduction

In this section, we examine supporting experimental evidence for some of the basic ideas encountered in this dissertation. Specifically, in Section 2, we showed that through the utilization of intensity beat signals at a detection plane, a spatial Fourier transform relation is derived with respect to the source-plane irradiance distribution. In Section 4, we showed that the Fourier transform relation between the source and detection planes using time-varying intensity beats of an optical source is identical to that derived in laser speckle theory[26,27] using a monochromatic formulation. Since these two theories are identical in their spatial transform relations, we will show first the results of unpublished laser speckle experiments performed by Peppers[28] which verify these relations.

As we have discussed in Section 4, the signal utilized in laser speckle theory (and by Peppers in his experiments) is time invariant, and, hence, can be recorded with a long exposure. Here, we will refer to this signal as the "dc speckle pattern." By analogy, the time-varying intensity signal of import to the intensity-interferometry formalism we will refer to as the "ac speckle pattern." In the latter half of this section, we will describe our own measurements of intensity fluctuations in a laser speckle pattern. By these experiments, we can infer the existence of an ac speckle pattern, the nature of its fluctuations, and its relation to the dc speckle pattern.

5.2 Experiments in Spatial Intensity Correlation

We describe now the intensity correlation experiments cf Peppers[28] which illustrate the transform relations given in Sections 2 and 4. The experimental configuration that he used is similar to that illustrated earlier in Figure 2.1. A helium-neon laser has been used to illuminate an opal-glass diffuser (to introduce spatial incoherence) followed immediately by an object; it consists of a 200-mesh grid of square holes outlined by a 1.22-nm circular hole in a metal plate. A photograph of this object is shown in Figure 5.1. This grid, along with the glass diffuser, was placed at plane 0 illustrated in Figure 2.1. At plane F, the resulting dc speckle pattern was recorded photographically and is shown here in Figure 5.2.
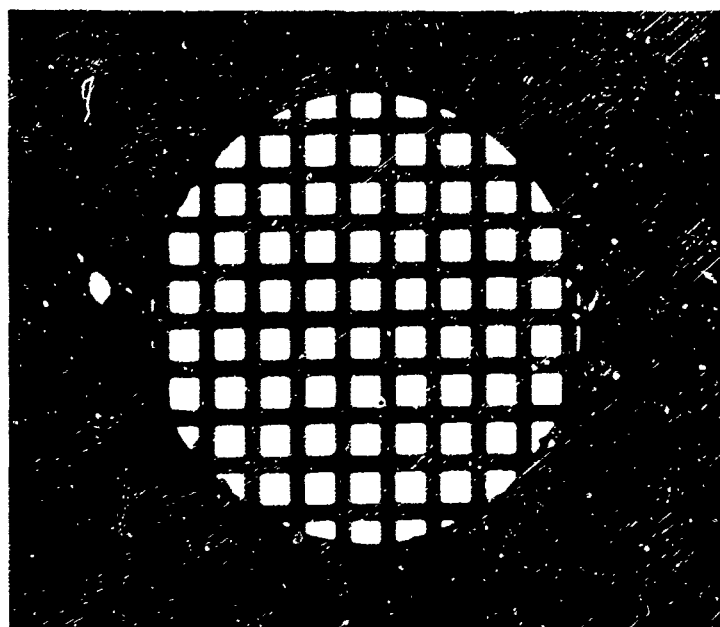
52

Figure 5.1 Object used for laser speckle recording.
A 1.22-mm circular hole outlines a 200-mesh grid.
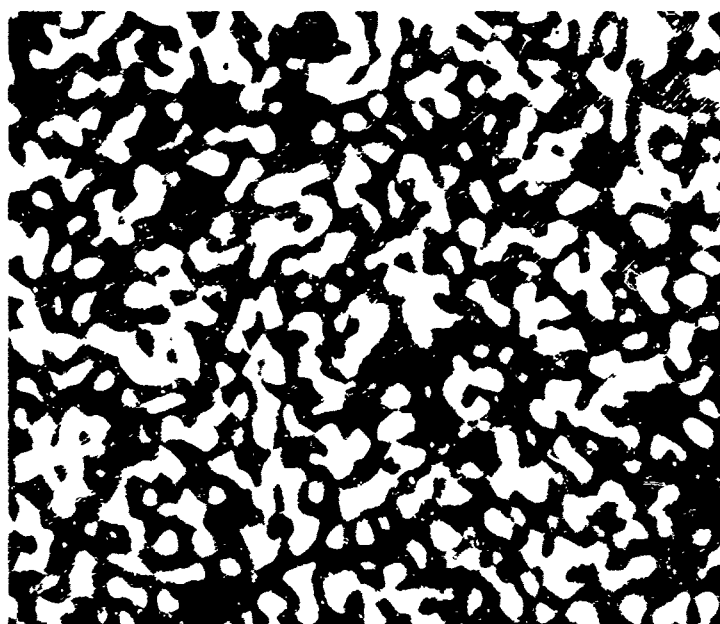
(Courtesy of N. A. Peppers[28])

Figure 5.2 Far-field speckle pattern of object
shown in Figure 5.1 with opal-glass diffuser.[28]

The photographic record made at plane F, Figure 2.1, was used to make a pair of positive transparencies in order to form the autocorrelation function given in Equation (4.6). In Figure 2.2, we illustrated a standard way in which an autocorrelation function can be formed by translating physically one transparency to all vector spatial lags $\underline{f}'$. An alternative approach, used by Peppers, is shown in Figure 5.3.
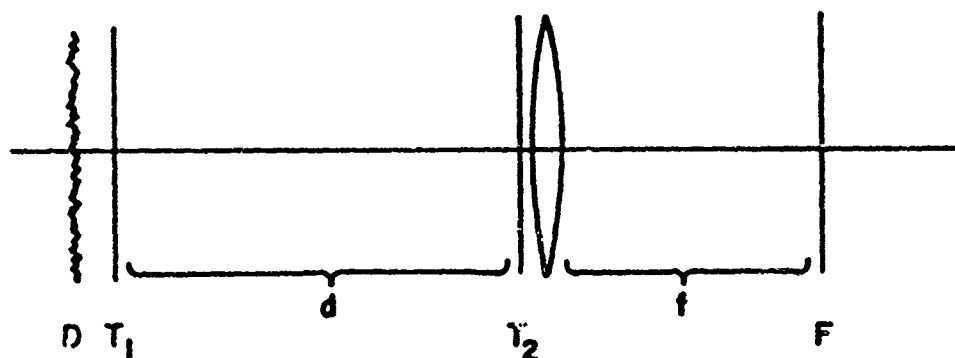
Figure 5.3 Optical system used to form the correlation of transparencies, T_1 and T_2. Collimated light impinges from the left onto diffuser, D. Distance between T_1 and T_2 is d, and f indicates the focal length of the lens. F denotes the film plane.

Collimated light from the left is diffused at plane D where the first transparency, T_1, is placed. At a distance d from the first transparency, a second identical positive, T_2, is positioned and followed directly by a lens of focal length f. At the focus of the lens, film (F) records the two-dimensional autocorrelation function. Reflection on the geometrical optics interpretation of this system reveals this operation as well as the equation governing the spatial magnification; in the film plane,

$$\underline{s} = f\underline{f}'/d, \qquad (5.1)$$

where $\underline{s}$ is the spatial lag in the film plane, f is the focal length of the lens, $\underline{f}'$ is the spatial lag between the transparencies, T_1 and T_2, and d is the distance between the two transparencies.

The results of this operation are shown in Figure 5.4 We note a central spot containing low-frequency information about the object centered among four side lobes, reflecting strong spatial-frequency content due to the periodicity of the 200-mesh grid. The signal illustrated in Figure 5.4 is the function given by Equation (4.6). It should be noted that the intensity relation of Equation (4.6) is similar to the expression in electric fields given by Equation (1.3). Peppers recorded the square of the electric field expressed by Equation (1.3) by using the Fourier transform apparatus of the kind illustrated in Figure 2.1 after
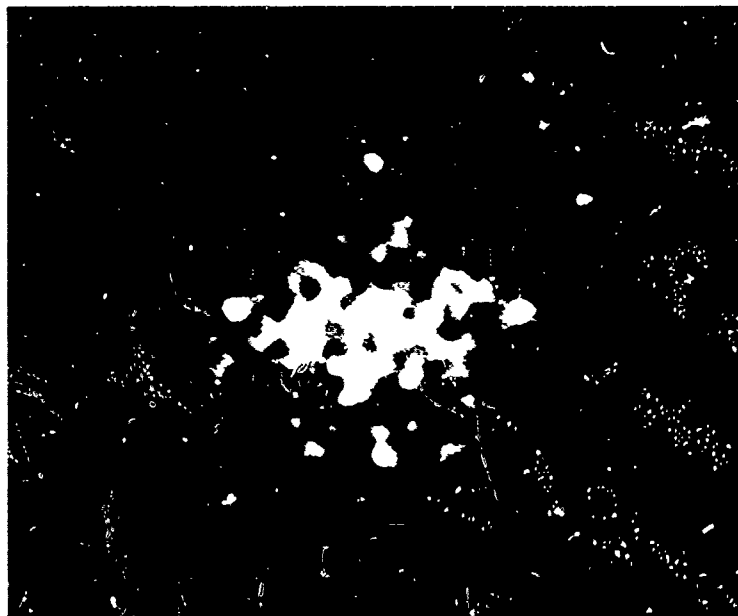
Figure 5.4   Optical autocorrelation of speckle pattern shown in Figure 5.2.[28]

first removing the ground glass at plane 0.   The result is presented in
Figure 5.5 and is to be compared with the function shown in Figure 5.4.
Except for the spatial noise of Figure 5.4, the two functions are similar
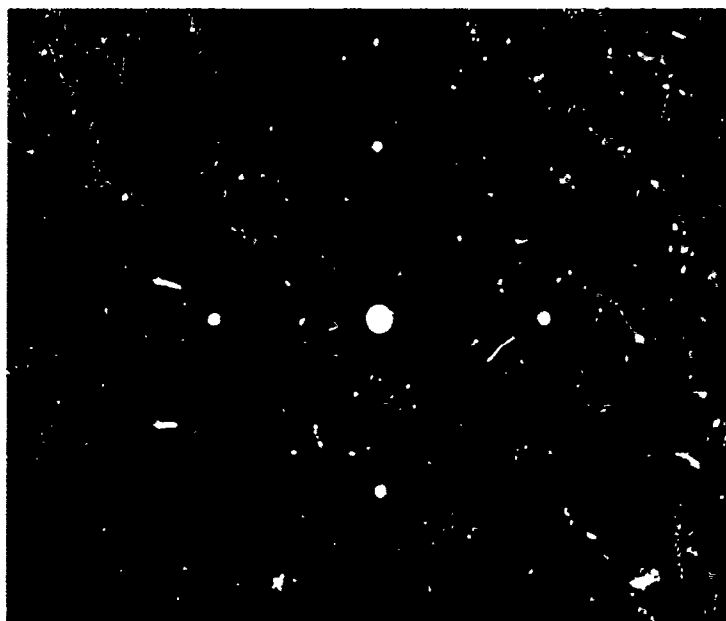in the manner indicated by Equations (1.3) and (4.6).

Figure 5.5   Diffraction pattern of object in Figure 5.1 made by
            configuration illustrated in Figure 2.1 after
            removal of optical diffuser at plane 0.[28]

55

In the previous chapter, the autocorrelation theorem was used by Goldfischer[26] to relate the Fourier transform of the source intensity autocorrelation [Equation (4.4)] to the equivalent expression of the squared modulus of the source intensity Fourier transform [Equation (4.6)]. Peppers illustrated this equivalence by the following operations. First, the source irradiance (Figure 5.1) was photographed and autocorrelated to form the object autocorrelation function (Figure 5.6). Next, both the intensity autocorrelation function (Figure 5.4) and the squared modulus of the diffraction pattern (Figure 5.5) were optically transformed to effect the Fourier inverse of the first operation of Equation (4.4); these results are shown in Figures 5.7 and 5.8, respectively. Although the signal quality of Figure 5.7 is somewhat poor, the similarity among these operations can be seen.

On the basis of these intensity correlation experiments, it appears that the spatial transform relations predicted by Goldfischer for the dc speckle pattern can be verified. We have shown in this dissertation the equivalence between the spatial transform relations for the dc and ac speckle signals. It remains now to show the specific relationship between these two speckle patterns. We examine this subject experimentally in the next sections.

5.3 Conditions for Coherence

Before examining laser speckle patterns experimentally, we find it useful to review the conditions for obtaining spatially fixed interference patterns. A discussion of these criteria, as well as detailed experiments into the nature of speckle patterns, has been given by Martienssen and Spiller.[29] We follow closely their development.

It can be asserted[29] that each oscillation mode of a source can interfere only with itself. Since the volume of an oscillation mode in phase space is h^3 (where h is Planck's constant), the Heisenberg uncertainty relation can be used to write the ranges in position (x,y,z) and momentum (p_x, p_y, p_z) for a photon in the mode, where

$$\Delta x \ \Delta p_x = h, \tag{5.2a}$$

$$\Delta y \ \Delta p_y = h, \tag{5.2b}$$

$$\Delta z \ \Delta p_z = h. \tag{5.2c}$$

If the mode propagates in the z direction, the uncertainty of the momentum in the x-z and y-z planes [per Equations (5.2a) and (5.2b)] can be expressed in terms of the angular apertures $2\Delta u_x$, $2\Delta u_y$ of the beam in the x-z and y-z planes. Using the relations $h/p = \lambda$ and $\sin\Delta u_x = \Delta p_x/p$, $\sin\Delta u_y = \Delta p_y/p$, we can write

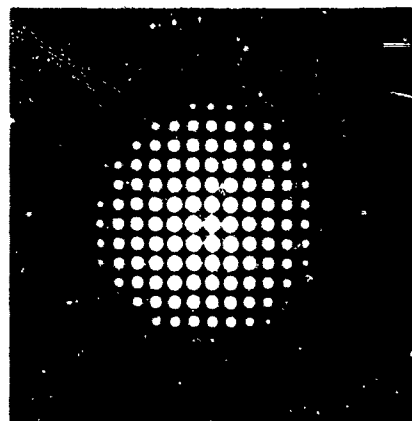Figure 5.6 Autocorrelation of object function illustrated in Figure 5.1.[28]

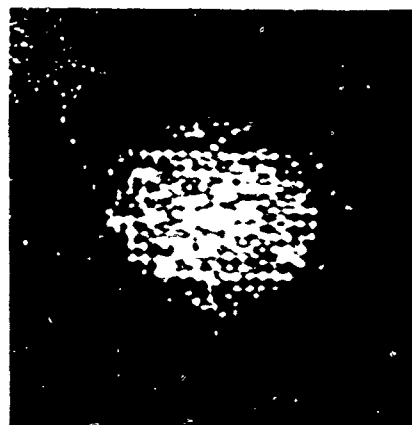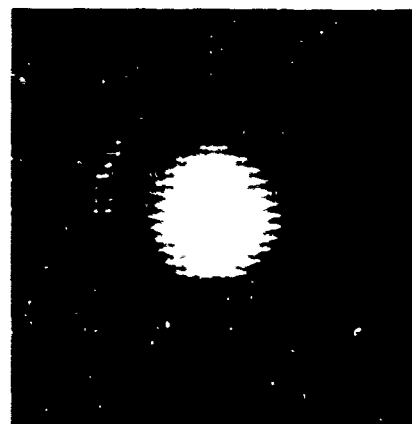Figure 5.7 Optical Fourier transform of signal function of Figure 5.4.[28]

Figure 5.8 Optical Fourier transform of signal function of Figure 5.5.[28]

$$\Delta x \, \sin \, \Delta u_x = \lambda, \tag{5.3a}$$

$$\Delta y \, \sin \, \Delta u_y = \lambda. \tag{5.3b}$$

Using $\Delta p_z = h\Delta\nu/c$ and $\Delta z = c\Delta t$, where $\Delta\nu$ is the frequency spread of the light and Δt is the time during which the beam is observed, Equation (5.2c) can be used to get

$$\Delta\nu \, \Delta t = 1. \tag{5.4}$$

The values of the angular apertures $2\Delta u_x$, $2\Delta u_y$ which fulfill Equations (5.3a) and (5.3b) are called the coherence angles, and the value of observation time Δt fulfilling the criterion of Equation (5.4) is called the coherence time. Angles less than the angular apertures define the conditions for spatial coherence, or

$$\alpha_x \ll \Delta u_x, \tag{5.5a}$$

and

$$\alpha_y \ll \Delta u_y. \tag{5.5b}$$

Observation times less than the coherence time Δt fulfill the condition for temporal coherence, or

$$T \ll \Delta t. \tag{5.6}$$

If the criteria of Equations (5.5a) and (5.5b) are met, a section of a light beam will experience no fluctuation in space, although, depending on the observation time T and the inequality expressed by Equation (5.6), it may experience fluctuations in time. In addition, if a light beam is observed in a time fulfilling the criterion of Equation (5.6) (is temporally coherent), then there will be no fluctuations in time; but if the observation area is large enough, there will be fluctuations in space.

5.4 Experiments in Temporal Intensity Fluctuations

Martienssen and Spiller[29] were apparently the first to suggest the use of a laser-illuminated rotating ground glass to model a thermal source with variable coherence time. Even with a laser, the finite width of its frequency spectrum implies some fluctuations in intensity. These fluctuations can be filtered using a detector with a slow response. If the laser illuminates a section of ground glass, the random phase variations introduced in the beam are similar to the phase mapping that would be observed over an incoherent source if the measurement were made in a time less than the coherence time. Thus the stationary ground glass corresponds to the case of infinite temporal coherence. By rotating the ground glass, the phase variations over the source can be made to change with a coherence time inversely proportional to the angular velocity of the ground glass.

This experimental approach was used by Martienssen and Spiller to repeat the Hanbury Brown - Twiss laboratory experiment in which the correlation of intensity fluctuations in a beam was examined as a function of detector separation [see Equation (1.21)]. We have duplicated that experiment using a setup illustrated in Figure 5.9. A Spectra-Physics Model 125 helium-neon laser is used to illuminate a section of ground glass that can be kept stationary or rotated by a motor. The far-field pattern is divided by means of a beam splitter and examined by two photomultipliers, one of which can be translated transverse to the optical axis. The outputs of the photomultipliers are fed through amplifiers with a dc block into an electronic correlator (Princeton Applied Research Correlator, Model 101). The cross-correlation of the two signals is observed by means of an oscilloscope readout.
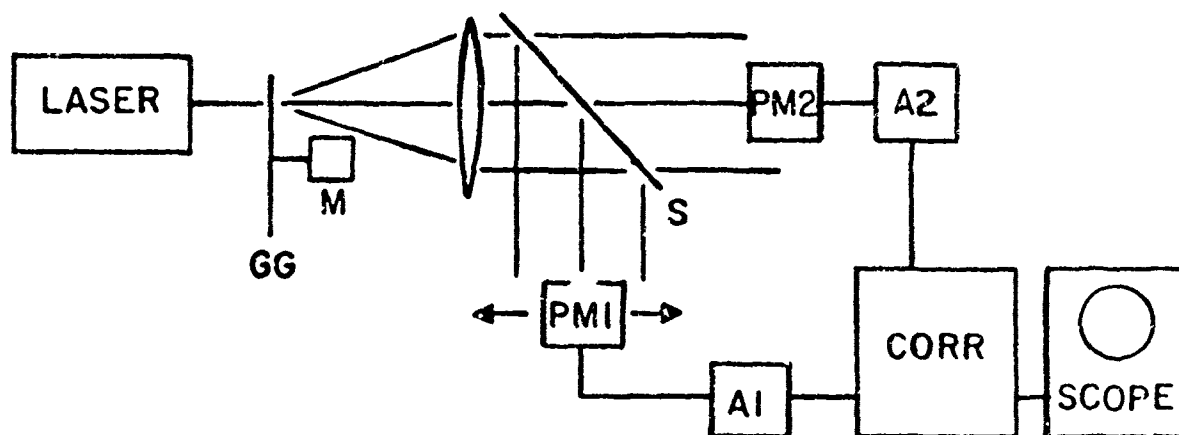
Figure 5.9 Experimental configuration for the correlation of temporal fluctuations within a laser speckle pattern. Ground glass (GG) can be spun by means of motor (M); beam splitter (S) divides speckle pattern into two images that are viewed by photomultipliers (PM1,PM2); outputs are fed through amplifiers (A1,A2) into electronic correlator and into display oscilloscope. Photomultiplier PM1 can be translated across the beam.

In Figure 5.10, we show the correlator output for the case of the rotating ground glass and complete alignment of the two photomultipliers. The correlation of electronic signals is shown as a function of time delay between the two signals. The integration time of the correlator is 15 s, and the maximum delay shown is 50 ms. The computed correlation time of the irradiance fluctuations can be shown to be on the order of 20 µs. Thus the correlation behavior of central interest is not resolved by the scale used in Figure 5.10. Because of the rotation of the ground glass, the correlation function is periodic. This periodicity, as well as the fine structure on the correlation function due to the non-ideal operation of the spun ground glass, can be easily removed by use of
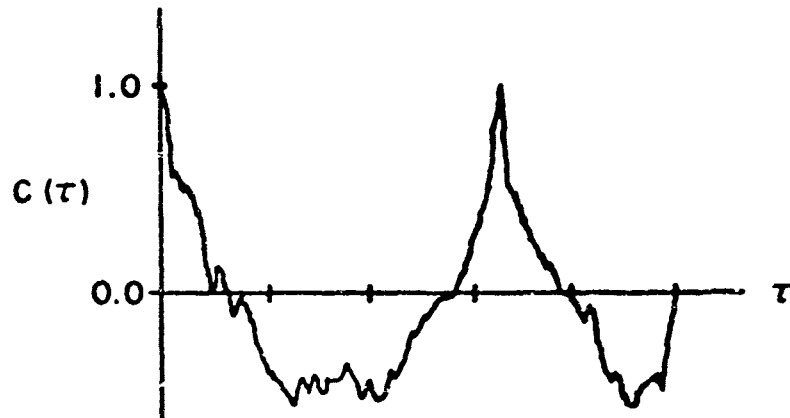
Figure 5.10 Oscilloscope trace of correlator output. Correlation C(τ) is plotted vs. time delay, τ, between fluctuating signal components. Both optical detectors viewed the same area of the laser speckle pattern. Each division along the τ axis corresponds to a time delay of 10 ms.

high-pass filters before the process of correlation. In the experiments that follow, the correlation lag (τ) scale was expanded to give the maximum (system tested) temporal resolution on the order of 5 μs. In addition, the following measurements make use of the correlation at zero time delay (origin of the correlation function).

We examined the correlation of intensity fluctuations as a function of detector separation. Figure 5.11 shows the results; the correlation is given versus spatial lag ($\underline{f}'$). The spatial correlation interval in the receiver plane is a function of the spot size on the ground glass; for the setup used the predicted interval is about 0.065 mm. The detector apertures were about 0.3 mm for reasons of detector efficiency in ensuing experiments. Thus the shape of the correlation is more a function of detector aperture than source function. The apparent correlation interval is about 0.3 mm. It can be seen that the results show a residual correlation level which is due to low-frequency components in the beam. These low frequencies were progressively eliminated using the high-pass capability of the amplifiers. The residual correlation was essentially gone after removal of fluctuations lower than 500 Hz. These results illustrate the predicted relation of Equation (1.21) and compare as well with the experiment of Martienssen and Spiller (Ref. 29, Figure 7).

The question posed in an earlier section involves the relation between the static (dc) and time-varying (ac) speckle patterns due to a laser source. The setup of Figure 5.9 was used to investigate this phenomenon by keeping the ground glass stationary and examining the temporal fluctuations due to the laser itself. The stability of this helium-neon laser is such that the intensity fluctuations compose only a small
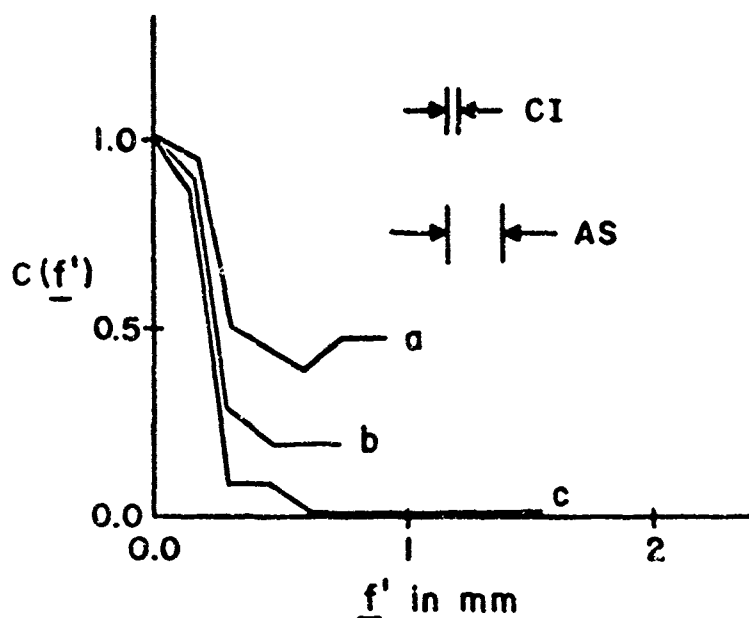
60

Figure 5.11 Normalized crosscorrelation of intensity fluctuations
vs. difference of detector positions ($\underline{f}'$) for the case of spinning
ground glass. Spatial correlation interval (CI) and detector
aperture size (AS) are shown. Coherence time of the radiation
~20 μs. Curves a, b, and c indicate high-pass filtering starting
at 1, 100, and 500 Hz, respectively.

fraction (< 1%) of the average intensity level. One might imagine that
the temporal mode fluctuations across the laser wave front are every-
where identical since the source is spatially coherent. In the far
field where the speckle pattern appears, the temporal intensity fluctu-
ations should be completely correlated; this concept can be stated
simply

$$I(\underline{x}_1, t) = A(\underline{x}_2) \; I(\underline{x}_2, t), \tag{5.7}$$

or the temporal fluctuations of intensity at one point in the speckle
pattern are identical to the temporal fluctuations at another point in
the pattern times a constant which depends on the average value of the
intensity at that point. This constant is, in fact, the dc speckle
pattern at that particular point.

The crosscorrelation function was measured as before but with the
ground glass stationary. For each spatial lag, the correlation at zero
temporal lag and the dc photocurrent on the movable detector were meas-
ured. We note that the intensity fluctuations due to the laser are a
full two orders of magnitude lower than the rotating ground glass fluc-
tuations. The photomultipliers were operating near the limit imposed
by shot noise; evidence for this observation is given by comparison of

61

the crosscorrelation of photomultiplier signals at zero spatial lag with
the autocorrelation of one signal. The autocorrelation is a factor of
two greater because of the correlation of noise; under crosscorrelation
the uncorrelated noise terms vanish. The correlation was normalized by
the dc value, and the results are shown in Figure 5.12. As before,
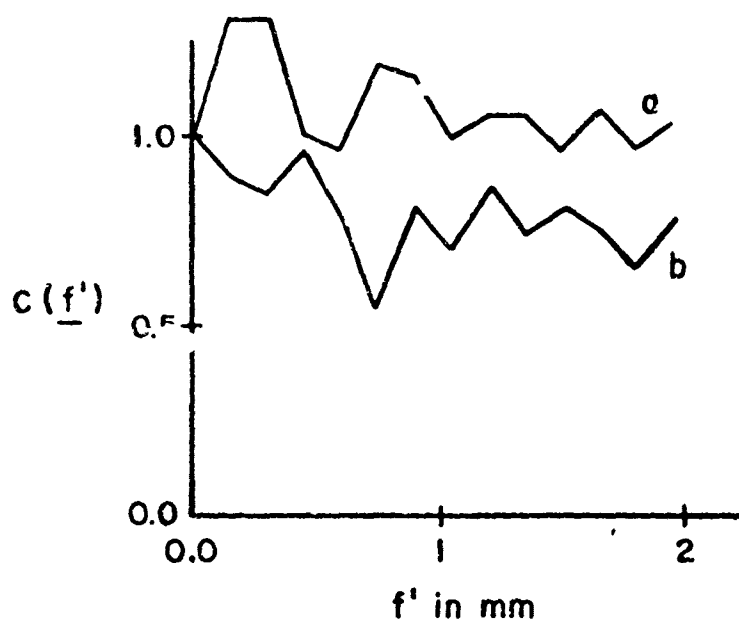

Figure 5.12 Normalized crosscorrelation of intensity fluc-
tuations vs. difference of detector positions ($\underline{f}'$) for the
case of static ground glass. Spatial correlation interval
and detector aperture size are shown in Figure 5.11.
Curves a and b indicate high-pass filtering of 500 and 1 Hz,
respectively.

high-pass filtering of 1 and 500 Hz was applied to the two data runs
shown. The detector aperture size and spatial correlation interval
remained the same. As can be seen, the temporal fluctuations are com-
pletely correlated for distances greater than forty times the spatial
correlation interval for this situation in which a spatially coherent
source illuminates a time-independent phase screen. Here, the ac speckle
pattern is identical to the dc speckle pattern and appears merely as a
fluctuation around the average (dc) value. On the average, then, in
this situation there is no gain by making a fast exposure, even if the
depth of modulation were somewhat greater than one percent.

It should be noted that this condition was anticipated earlier above
Equation (2.32). There it was argued that all areas of the scatterer
see the same mode history (i.e., the source is spatially coherent) and
that, therefore, the mode fluctuation of the laser would simply be seen

62

as a variation in total received power from one sample to the next. The measurements of Figure 5.12 bear out this concept.

5.5 Summary and Conclusions

In this chapter, we have seen the way in which the far-field speckle pattern of a spatially incoherent source can be related to the intensity over the source itself. We have also discussed the conditions for spatial and temporal coherence and investigated, experimentally, the correlation of temporal fluctuations in laser speckle patterns. It can be seen that laser speckle theory[26,27] forms the limiting case in intensity interferometry in which the coherence time of the source becomes large and for which the averaging is accomplished in a spatial sense. At the opposite extreme is found the Hanbury Brown - Twiss experiment in which an incoherent source is monitored by means of temporal fluctuations averaged along the time axis. We have seen [in Equation (1.20)] that many of the beat frequencies in the carrier wave are not useful, practically, because of the limitations in detector frequency response. This dissertation bridges these limiting cases by formulating the case of quasimonochromatic radiation (finite coherence time) detected and averaged in the spatial domain.

To elucidate the ultimate equivalence among these approaches, we turn to Figure 5.13. We have represented an ensemble of similar configurations of source-detector planes. We imagine the field-amplitude distribution across each plane to be identical as well as the two detection points in the receiver planes. The Hanbury Brown - Twiss case (quasimonochromatic source, temporal averaging) is taken first. We let each member of the ensemble represent an intensity measurement made in a time less than the coherence time of the radiation. The phase structure over each source surface is therefore frozen, but statistically independent from one another. Hanbury Brown and Twiss started by forming the product of intensities at the two detection points in, say, the ith member. They, of course, wanted the ensemble average of that product and, through the assumption of temporal stationarity and ergodicity, sought the equivalent operation by means of a time average. This can be visualized by allowing the member j to represent the identical source amplitude now exhibiting a new phase structure due to the evolving temporal mode histroy over the source. As many samples are averaged in time, the function approaches the ensemble average.

In the case of spatial averaging, the ith sample can be taken as a spatial recording of intensities in the x-plane over a time short compared with the coherence time of the radiation. Two points within the pattern can be sampled to form the product but, again, it is the ensemble average that is desired. Here, through the assumption of spatial stationarity (and a sufficiently large area of spatial averaging), the spatial average is assumed equivalent to the ensemble average.
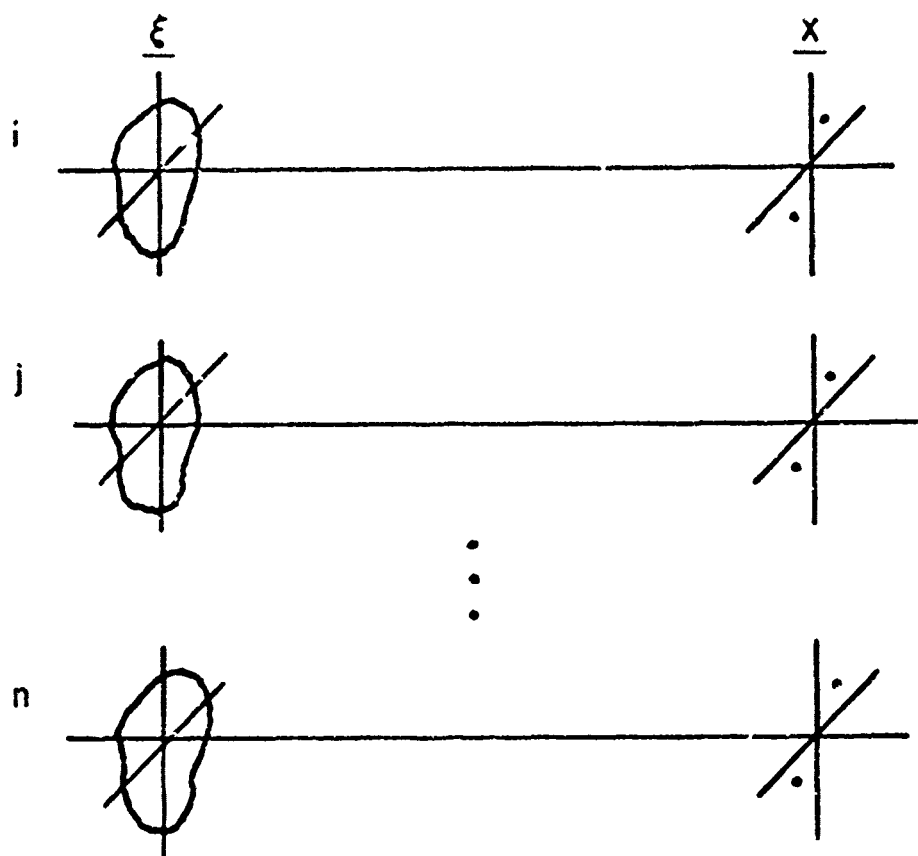
Figure 5.13 An ensemble of similar experiments. Source ampli-
tude and receiver points are identical. Random phase variations
over each source plane are statistically independent.

We note that all the schemes involving intensity correlation require
a random phase structure across the source. It is achieved naturally
for an incoherent source, and for a spatially coherent laser it can be
accomplished by use of a diffusing glass. We note that this condition
is described analytically by the exponential term of Equation (2.31).
This term is written sufficiently general to include phase perturbation
due either to spatial surface roughness or to temporal mode difference.
It should be noted that a suitably prepared broad-band laser might be
utilized without ground glass if the temporal mode structure could be
sufficiently varied in a statistically stationary way over the scattering
surface.

We note again, as we did at the beginning of Section 1, that the
focus of primary interest in optical imaging is the spatial domain. How-
ever, we have seen that the ability to detect intensity fluctuations and
the manner in which an average is finally taken rests in a most crucial
way with the nature of the temporal statistics of the radiation.

64

ACKNOWLEDGMENT

REFERENCES

1. R. Hanbury Brown and R. Q. Twiss, *Phil. Mag.* 45, 663 (1954).

2. M. J. Beran and G. B. Parrent, Jr., *Theory of Partial Coherence* (Prentice-Hall, Englewood Cliffs, 1964), p. 172.

3. R. Hanbury Brown and R. Q. Twiss, *Proc. Roy. Soc.*, Ser. A, 242, 300 (1957), and Ser. A., 243, 291 (1957). These papers appear in *Coherence and Fluctuations of Light*, Vols. I and II, L. Mandel and E. Wolf, eds. (Dover, New York, 1970).

4. J. W. Goodman, *Progress in Optics*, Vol. VIII, E. Wolf, ed. (North Holland, Amsterdam, 1970), p. 21.

5. E. Wolf, *Phil. Mag.* 2, 351 (1957).

6. H. Hodara, *Proc. IEEE* 53, 696 (1965).

7. M. Born and E. Wolf, *Principles of Optics*, 4th ed. (Pergamon, Oxford and New York, 1970), Ch. 10.

8. D. L. Fried, *J. Opt. Soc. Am.* 57, 169 (1967).

9. G. Magyar and L. Mandel, *Nature* 198, 255 (1963).

10. H. Gamo, *Proc. Symp. on Electromagnetic Theory and Antennas*, Copenhagen, June 1962 (Pergamon, New York, 1963), p. 809.

11. E. W. Marchand and E. Wolf, *J. Opt. Soc. Am.* 62, 379 (1972).

12. L. Mandel and E. Wolf, *Rev. Mod. Phy.* 37, 231 (1965).

13. G. J. Troup, *Proc. IEEE* 53, 1732 (1965).

14. D. Middleton, *Introduction to Statistical Communication Theory* McGraw-Hill, New York, 1960), p. 343.

15. A. Walther, *J. Opt. Soc. Am.* 58, 1256 (1968).

16. K. Miyamoto and E. Wolf, *J. Opt. Soc. Am.* 52, 625 (1962).

17. J. W. Goodman, *Proc. IEEE* 53, 1688 (1965).

18. R. E. Kinsly, *J. Opt. Soc. Am.* 62, 386 (1972).

19. E. Wolf, *Proc. Phys. Soc.* (London) 80, 1269 (1962).

20. P. Roman and A. S. Marathay, *Nuovo Cimento* 30, 1452 (1963).

REFERENCES (CONT.)

21. A. Waither, *Opt. Acta* <u>10</u>, 41 (1963).

22. H. Gamo, *J. Appl. Phy.* <u>34</u>, 875 (1963).

23. C. L. Mehta, *J. Opt. Soc. Am.* <u>58</u>, 1233 (1968).

24. R. Bracewell, *The Fourier Transform and Its Applications* (McGraw-Hill, New York, 1965).

25. H. W. Wessely and J. O. Bolstad, *J. Opt. Soc. Am.* <u>60</u>, 678 (1970).

26. L. I. Goldfischer, *J. Opt. Soc. Am.* <u>55</u>, 247 (1965).

27. R. B. Crane, *J. Opt. Soc. Am.* <u>60</u>, 1658 (1970).

28. N. A. Peppers, Stanford Research Institute, private communication.

29. W. Martienssen and E. Spiller, *Am. J. Phys.* <u>32</u>, 919 (1964).